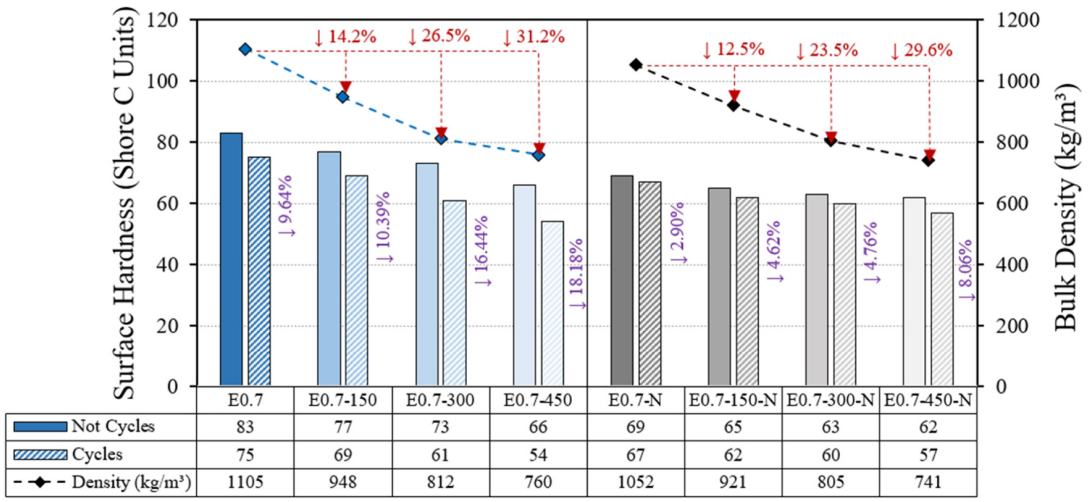

Fig. 7. Bulk density and Shore C surface hardness for different plaster composites.

decrease in density is even more significant in those composites with the addition of ELT textile fibres. Likewise, surface hardness is lower when the amount of recycled material added is higher, both in the reference samples and in the samples subjected to accelerated ageing cycles. In all the samples studied, surface hardness values higher than 50 Shore C units were obtained after the cycles. Compared to other studies and considering their best results with the addition of granulated EPS waste (710 kg/m^3 and 50 Shore C units) [53] or crushed XPS (1170 kg/m^3 and 60 Shore C units) [14], the results obtained by adding EPS waste in solution with or without ELT textile fibre were higher on average in all the samples.

Figs. 8 and 9 show the results of the mechanical bending and compression tests for the samples subjected to wet-chamber cycling and their comparison with the reference series.

All the flexural strength values presented in Fig. 8 for the different samples analysed are well above the minimum set by the standards. Flexural strength decreases progressively as the amount of recycled material added to the composites increases, being slightly higher in the plaster materials without ELT textile fibres and containing only the recycled EPS solution. All the samples subjected to humidity-dryness cycling recorded lower flexural strengths than their reference counterparts without cycling. However, and innovatively, the decrease in strength caused by cycling compared to the reference samples is reduced in those with higher recycled content, thus supporting the suitability of this material for application in false ceiling panels for wet rooms.

Like flexural strength, the minimum threshold set by the standards was exceeded in all the samples tested mechanically in compression, as illustrated in Fig. 9. This property records a more severe effect caused by the humidity-dryness cycles, as the samples in all the cases tested recorded mechanical strengths 23 % lower than their reference series. In this case, and unlike flexural strength, the

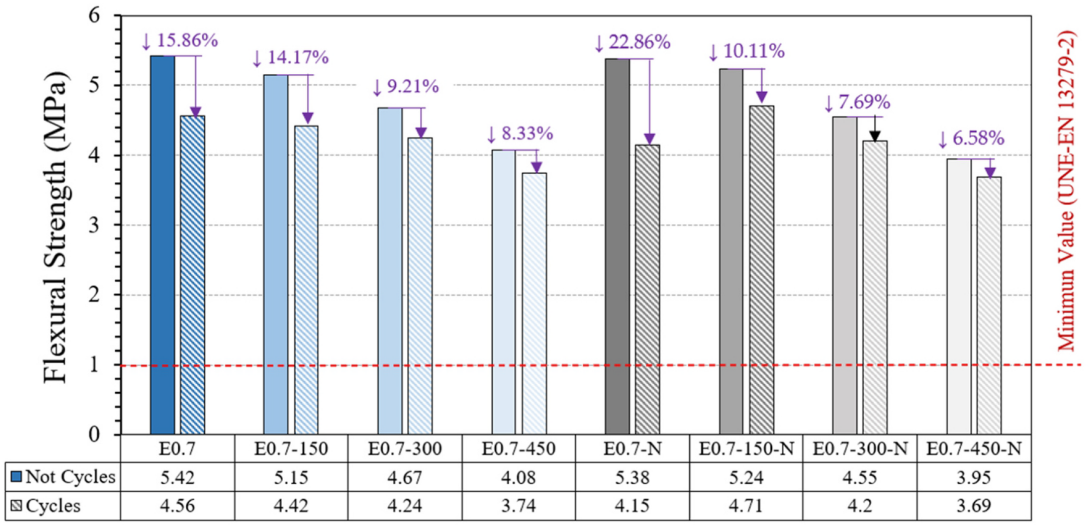

Fig. 8. Flexural strength of plaster composites subjected to wet-chamber cycling, and comparison with the reference series.

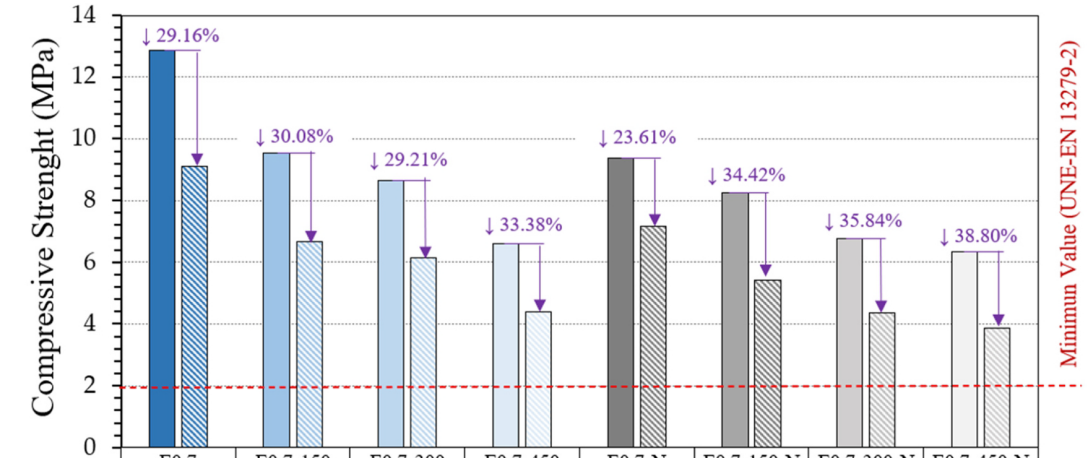

Fig. 9. Compressive strength of plaster composites subjected to wet-chamber cycling, and comparison with the reference series.

greater the amount of original plaster material replaced by recycled EPS solution (with and without fibres), the greater the decrease in the compressive strength of the samples when subjected to the effect of the humidity-dryness cycles.

Compared to prior studies, reference flexural strengths (4.08 MPa and 3.95 MPa) and compressive strengths (6.59 MPa and 6.34 MPa) are higher even in the composites with the most EPS residue in solution added (E0.7-450 and E0.7-450-N). It is worth mentioning the study by Del Río et al., where the best results obtained by adding shredded EPS waste were 1.81 MPa in bending and 3.11 MPa in compression [14]; as well as the study by San Antonio et al., using shredded XPS waste, which achieved the best results for their plaster composites of 2.32 MPa in bending and 3.15 MPa in compression [54]. Regarding the results obtained in wet-chamber cycles, Vidales et al. have added plastic waste in 50 % by weight of shredded cable and obtained 2.23 MPa in bending and 3.80 MPa in compression after two wet-chamber cycles [34]. For the same test, Leiva has obtained 3.15 MPa in bending and 6.20 MPa in compression after adding 10 % rice husk residue to plasters [55]. The samples in this research have clearly performed well against humidity, maintaining a mechanical capacity after ten aggressive wet-chamber cycles that is higher than other research studies.

Finally, in Fig. 10, SEM images have been obtained for some of the most representative samples of the series produced. These images help to understand the inner microstructure of the prepared plaster composites, as well as the interaction between the dihydrate crystals commonly formed in gypsum materials and the added residues [56]. Images have been taken for samples E0.7-450; E0.7-N; E0.7-450-N, as they are considered representative of the set of dosages taken during the experimental campaign.

Fig. 10(a) shows a magnified image of a pore formed in the matrix of the E0.7-450 composite. This porous structure, in turn, is responsible for the lower density with respect to the E0.7 reference plasters. However, the needle-shaped crystals characteristic of the dihydrate formed during the setting and hardening process of gypsum-based composites can be seen [57]. In turn, Fig. 10(b) shows another pore on the same sample, this time covered by a thin plastic film that corresponds to the dissolution of the EPS waste once solidified. This plastic coating has already been observed in other investigations [58] and helps to improve the mechanical behaviour of plasters subjected to severe humidity-dryness conditions.

Fig. 10(c) is obtained from sample E0.7-N, which has only ELT textile fibre residues. The needle shape of the dihydrate crystals is more pronounced, similar to that obtained in past studies [59]. In addition, the image shows the excellent cohesion of the matrix, with the recycled fibres being fully embedded and well bonded, which has a positive impact on the flexural mechanical behaviour [60]. Finally, Fig. 10(d) corresponds to sample E0.7-450-N, with good fibre-matrix adhesion, and this time the plaster crystals are shorter and wider than for the sample without EPS dissolution (E0.7-N), as already observed in another study in which EPS nanoparticles in solution were used to improve the thermal insulation capacity in lightened gypsum composites [61].

3.2. Simulation results

3.2.1. Factory-transport loading process

The first step is the simulation of the manual movement and productivity of the workers in a factory of prefabricated boards of a standard size of 40 × 30 × 1.5 cm, for their possible grouping by batches prior to their distribution. The developed composites involve a product redesign by modifying the processing of traditional plaster materials, replacing part of the original natural resources with recycled raw materials that would otherwise undergo slow and costly environmental degradation in landfills [62]. The incorporation of these product innovations in turn decreases the final weight of the precast plasterboards, which is reflected in an increase in an employee's normal production rate.

Fig. 11 shows the percentage distribution of time spent by each worker during the board loading process from factory to final

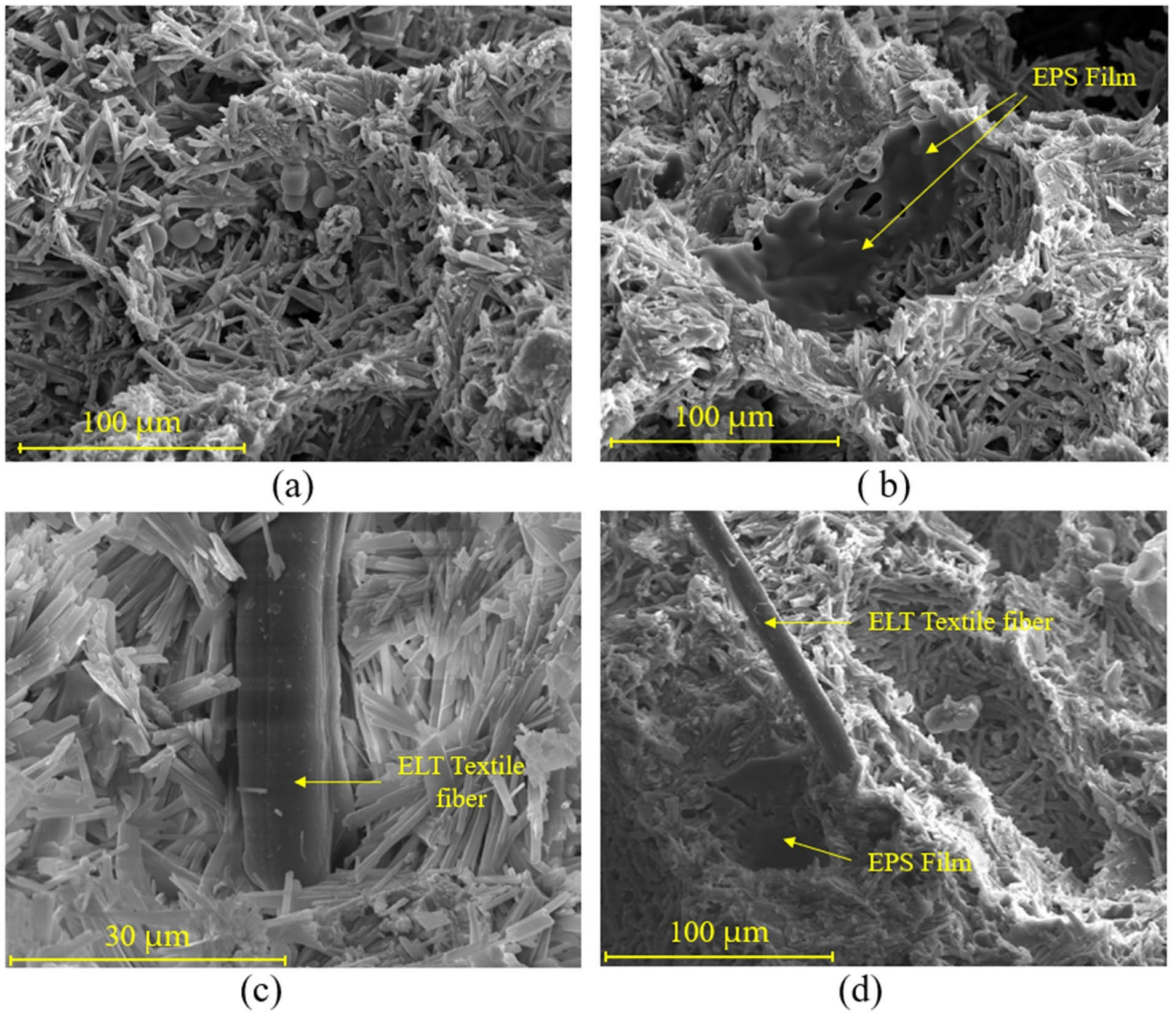

Fig. 10. SEM: (a) and (b) Sample E0.7-450, magnifications × 500; (c) Sample E0.7-N, magnifications × 2000; (d) Sample E0.7-450-N, magnifications × 500.

customer. The FlexSim parameterisation of this manual transport process is parameterised according to a Poisson distribution with mean $\mu = 10$ speeds. No process failures are considered and a constant work rate is assumed, dismissing any possible musculoskeletal injuries or a reduction in individual performance during a continuous eight-hour working day. The kinematics of the worker when picking up the items (acceleration) and putting them down (deceleration) are estimated at 1 m/s^2. In parallel, based on ergonomic criteria and the prevention of occupational hazards, it is understood that the speed of the manual transport of plasterboards will be greater in the case of lower density compounds. In a simplified way, an inversely proportional relationship can be assumed between speed and mass of the board transported (see Table 3), which also shows the productivity in units transported per day by each worker.

Today's fluctuating market dynamics and the uncertainty in order demand highlight the necessity of introducing more sustainable and efficient redesigns in traditional building materials, providing companies with greater flexibility and adaptability [63]. As noted in Table 3, the simulation records a progressive increase in productivity (units processed/day) as the amount of recycled raw material added to the precast composition increases. The productivity of the warehouse processing of the lightest boards with E0.7-450-N dosage is 9.2 % higher than that of traditional plasters (E0.7). These findings highlight the positive impact derived from the lightening of traditional prefabricated products by means of this method of recovery of EPS waste and ELT textile fibres. This improvement is in line with other research reporting that the introduction of innovations for the development of environmentally sustainable products is a key element for business performance [64].

The aims of warehouse management are to increase productivity and accuracy, reduce inventory costs, and satisfy the interests of the firm's stakeholders [65]. Accordingly, Fig. 11(b) shows that as the final weight of the plasterboards is reduced by adding the recycled EPS solution, the percentage of time spent on empty and loaded displacements decreases compared to the reference boards (E0.7). The same reasoning applies to boards with additional ELT textile fibre. Our simulation therefore suggests that warehouse

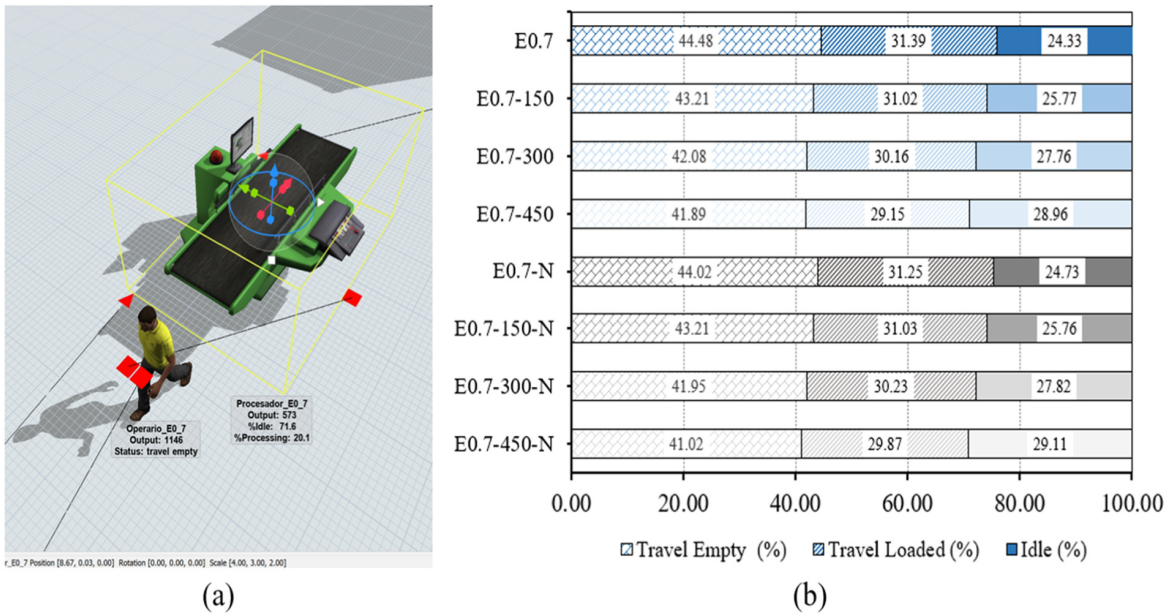

Fig. 11. (a) Image of the simulation of the factory-transport loading process; (b) Percentage distribution of the time spent on each activity in the factory during the loading process.

Table 3
Simulation parameters for each type of board and their estimated productivity.

Series	E0.7	E0.7-150	E0.7-300	E0.7-450	E0.7-N	E0.7-150-N	E0.7-300-N	E0.7-450-N
Mass (kg)/Plate (40 × 30 × 1.5 cm)	1.990	1.706	1.462	1.368	1.894	1.658	1.500	1.334
Operator speed (m/s)	1.18	1.22	1.25	1.26	1.19	1.23	1.25	1.27
Productivity (units/day)	71.63	74.13	75.54	78.16	72.51	74.97	76.63	78.91

employees may work more comfortably and perform their tasks more sustainably when transporting the newly developed lightweight prefabricated elements. This effect might have a positive impact on workers' health and well-being, as well as on the organisation as a whole, as it can increase the factory's performance. Likewise, the increased downtime can be used for support tasks at other points in the supply chain, such as inventory control, process improvement, and maintenance tasks, all to the company's ultimate benefit.

3.2.2. Impact on transport and CO_2 emissions

Figs. 12 and 13 show the findings obtained from the simulation of unit consumption (litres/board) and CO_2 emissions derived from the distribution of the new prefabricated products, which affect not only the organisation's bottom line, but also the greenhouse gas emissions attributed to the product's carbon footprint, and which affect society as a whole. The following initial assumptions were considered in the parameterisation of this simulation:

- Typical journey of 100 km for each means of transport used, with a diesel cost in Spain of 1.817 €/litre.
- Three distinct means of transport, whose maximum useful loads and volumes, as well as the average consumption in litres per 100 km of their diesel engines, are as follows: van: 1400 kg; 9.3 m^3; 11 l/100 km; lorry: 12,000 kg; 45 m^3; 27 l/100 km, and trailer: 25,000 kg; 83 m^3; 40 l/100 km.
- k-factor for diesel consumption in l/100 km•100 kg, average transport consumption in l/100 km and average emissions in $mgCO_2$/km, according to Spain's Ministry of Transport, Mobility and Urban Agenda [66].

Figs. 12 and 13 show that the unit consumption (litres/board) is reduced as the amount of recycled material introduced into the precast elements increases. Thus, replacing the original plaster material with dissolved EPS waste and adding ELT textile fibres reduces transportation logistics costs. This unit cost is further reduced with larger vehicles because of the increasing number of boards that can be transported on the same journey without exceeding the maximum permitted load. This reduction in costs represents a significant financial amount when considering economies of scale and the bulk displacement of elements from the storage centre.

A streamlined distribution process entails reducing the quantity and toxicity derived from the delivery of raw materials from the depot to the final destination and, as far as possible, reducing the costs incurred by this activity [67]. Logistics activities increase

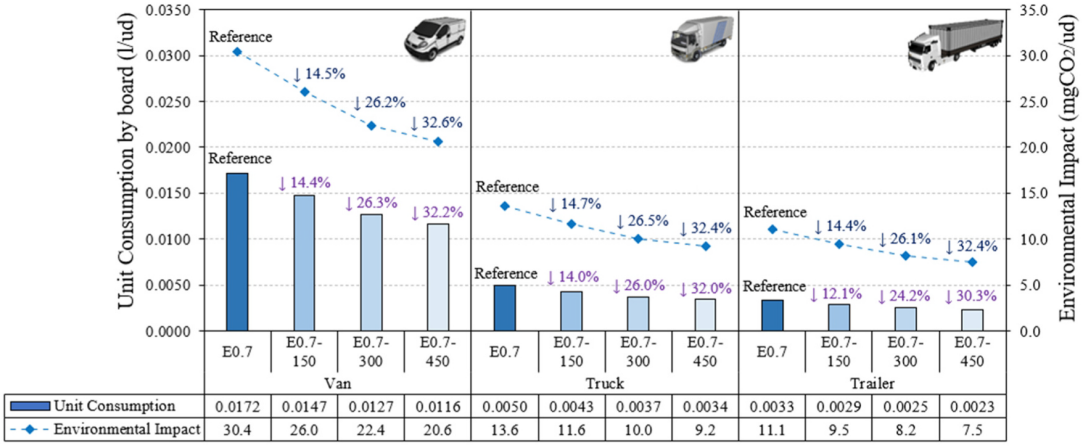

Fig. 12. Simulation results of unit consumption and CO_2 emissions in different transport scenarios for compounds without ELT textile fibres.

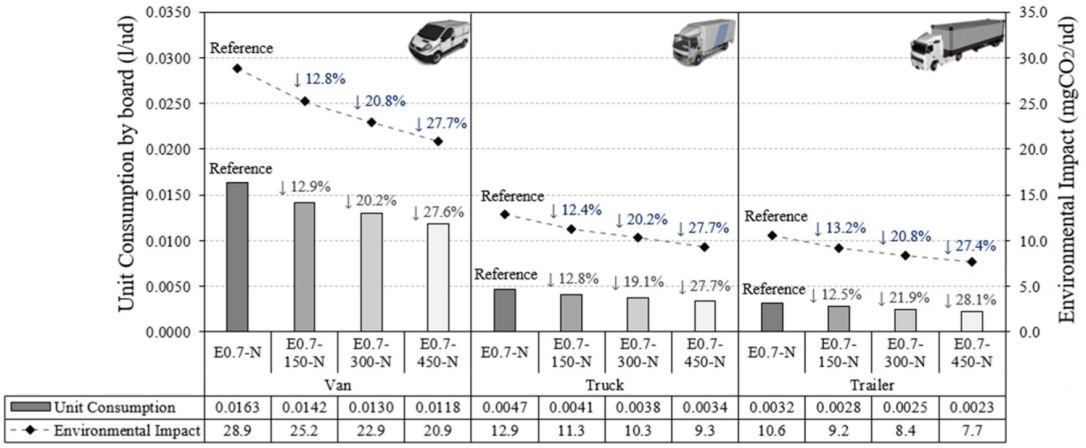

Fig. 13. Simulation results of unit consumption and CO_2 emissions in different transport scenarios for compounds with ELT textile fibres.

industrial and environmental emissions, and the onus is on the manufacturer to reduce the environmental impact at the end of their products' life cycles through an efficient design that decreases the consumption of natural resources and minimises environmental emissions [68]. The findings of the simulation show the potential application of the new products developed here, which may

Table 4
Statistical analysis for the difference of means between the mechanical characterisation results obtained for the wet-chamber cycled samples and the control samples.

Analysis of Variance (ANOVA)											
Surface Hardness (Shore C unit)				**Flexural Strength (MPa)**				**Compressive Strength (MPa)**			
Solution		Tyre		Solution		Tyre		Solution		Tyre	
p-value: 0.0509		p-value: 0.0000		p-value: 0.0000		p-value: 0.9871		p-value: 0.2784		p-value: 0.4247	
Multiple Range test for Wet-Chamber Cycles (Factor: Solution)											
Surface Hardness (Shore C unit)				**Flexural Strength (MPa)**				**Compressive Strength (MPa)**			
Level	Mean	Sigma	HG	Level	Mean	Sigma	HG	Level	Mean	Sigma	HG
0	5.33	0.8368	X	450	0.30	0.0509	X	450	2.33	1.5934	X
150	5.67		X	300	0.39		X	300	2.48		X
300	7.67		XX	150	0.62		X	150	2.86		X
450	8.33		X	0	1.04		X	0	6.28		X
Multiple Range test for Wet Chamber (Factor: Tyre)											
Surface Hardness (Shore C unit)				**Flexural Strength (MPa)**				**Compressive Strength (MPa)**			
Level	Mean	Sigma	HG	Level	Mean	Sigma	HG	Level	Mean	Sigma	HG
TF	3.5	0.5917	X	TF	0.588	0.0360	X	NF	2.837	1.1267	X
NF	10.0		X	NF	0.589		X	TF	4.137		X

contribute to the economic growth of organisations, without compromising the sustainable development of the construction industry. Figs. 12 and 13 show a progressive decrease in atmospheric CO_2 emissions as the amount of recycled raw material in the plaster composites increases, thus combining circular economy criteria in the manufacturing process of new building materials with the sustainable mobility included in the European Green Pact. This effect is even more beneficial, considering that the building industry is responsible for about 8 % of global atmospheric CO_2 emissions and generates around 7.0 billion tons of solid waste worldwide [69,70].

4. Statistical discussion of results and business impact

Table 4 presents a statistical discussion of the results obtained in the mechanical characterisation tests involving surface hardness, flexural strength, and compressive strength. The differences obtained between the mean values recorded by the reference samples without cycles and the results obtained by testing the samples subjected to ten humidity-dryness cycles are compared. An Analysis of Variance (ANOVA) has been conducted, considering the two factors included in this study: dissolution of EPS waste (Solution) and incorporation of ELT textile fibres (Tyre). Nine values were taken for each one of the properties. The Solution factor has four levels: 0, 150, 300 and 450, depending on the content of EPS waste solution; and the Tyre factor has two levels: incorporation of textile fibres (TF) or not (NF). A multiple range test has also been carried out to identify the existence of possible homogeneous groups among the levels included in this research. The diagnosis of the model has been checked, guaranteeing compliance with the requirements of independence, normality, and homoscedasticity of the residuals, which confirm the experiment's robust design.

Table 4 shows that the only statistically significant factor for surface hardness was the addition of ELT textile fibre with a p-value of 0.0000 ($p < 0.05$). The homogeneous group analysis reveals statistically significant differences between the reduction in surface hardness recorded by the samples without ELT textile fibre and those with this waste, with the latter recording a poorer performance. In the case of flexural strength, the only significant factor obtained was the content of recycled EPS solution (p-value of 0.0000). After the analysis of homogeneous groups, the loss of flexural strength after subjecting the samples to humidity-dryness cycles is more pronounced the higher their residual EPS content. Finally, no statistically significant differences were found in the decrease in compressive strength regardless of the type of recycled raw material added.

Nowadays, firms are striving to increase their competitiveness through product customisation, high quality, cost reductions, and speed-to-market. A new lightweight plaster material has been proposed here that is specifically designed for application in residential wet rooms. As an example, a false ceiling design is shown in Fig. 14 using prefabricated panels made with this material, which stands out for being lighter than traditional plaster composites and for its simple assembly. These prefabricated products involve a production process that is committed not only to the reincorporation of USW, but also provides other advantages and benefits from an economic viewpoint, as a direct result of a more efficient use of raw materials and resources, the optimisation of cost-saving production processes, and higher worker productivity.

Various simulation hypotheses have been put forward for extrapolating the economic results and environmental impact derived from these products' distribution. An adequate organisation of storage processes translates into lower logistics costs, functionality of operations, and a higher level of efficiency [71]. The simulation focused only on road transport, as it is the most flexible and most widely used for the distribution of building materials. Thus, an effective distribution management programme can make the difference between the success and failure of a supply chain, and it is the ultimate responsibility of construction companies to design networks that meet customer expectations in terms of rapid response, product-service quality, and environmental impact.

Finally, the building material developed here has potential sources of competitive advantage during its supply process because of its application in the production of prefabricated panels and boards:

- Cost reduction: reducing fuel consumption in bulk transport.

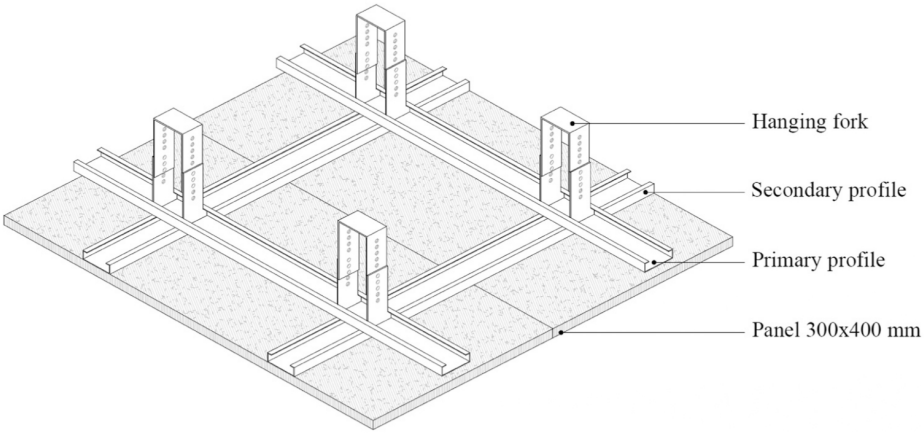

Fig. 14. Design of a false ceiling using prefabricated board in the simulation.

- Rapid response: shortening product preparation times for subsequent distribution thanks to the lighter weight of the prefabricated products. This improves the service provided to the customer, increasing the flexibility and speed of delivery.
- Differentiation: a novel product made under circular economy criteria, with a marked environmental nature that generates value added for this type of board and panels that can be perceived by the customer. In addition, the reduction in CO_2 emissions associated can also be used to obtain green labels that distinguish these eco-friendlier products.

5. Conclusions

The materials tested and the dosages used in this study comply with the requirements of the current reference standard UNE-EN 13729-2 [45], with all the samples exceeding the minimum threshold of 1 MPa of flexural strength and 2 MPa of compressive strength, even after being subjected to ten severe humidity-dryness cycles. Although repeated humidity-dryness cycles are detrimental to the mechanical behaviour of the materials produced, the mechanical performance obtained was superior to that reported by other studies producing plaster composites under circular economy criteria. The most significant cases are E0.7-450 and E0.7-450-N plasters, reducing the consumption of original raw materials by 27 % and 28 % respectively, and lightening the weight of the prefabricated products by 31.2 % and 33.0 % each with respect to the traditional E0.7 plaster.

On the other hand, the results of the simulation conducted in our study show that productivity can be improved in the process of loading and unloading stock because the new prefabricated product is lighter. In addition, our findings show that the unit consumption ratio of 'litres/board' decreases as the amount of recycled material added increases. This results in cost savings in terms of transport and a reduction in atmospheric CO_2 emissions, particularly when considering the potential achievement of economies of scale in the manufacturing process of this novel product. These findings support the excellent application possibilities of this novel product for use in the manufacture of prefabricated boards and panels for wet rooms, catering for a fast, efficient assembly/distribution process and a better use of existing resources.

A main limitation of this research is that the simulation focuses solely on the logistics process of distributing the final product, taking into account the savings in transportation and the decrease in CO_2 equivalent. Future research should consider the analysis of the complete life cycle of this type of product. This analysis, which is beyond the scope of the current study, could provide relevant information for building companies and could be used as a differentiating mark when obtaining potential sources of competitive advantage in the sector.

CRediT authorship contribution statement

Alicia Zaragoza-Benzal: Conceptualization, Methodology, Software, Formal analysis, Investigation, Data curation, Writing – original draft, Writing – review & editing. **Daniel Ferrández:** Conceptualization, Methodology, Formal analysis, Investigation, Writing – original draft, Writing – review & editing, Visualization, Supervision, Project administration, Funding acquisition. **Jorge P. Díaz-Velilla:** Methodology, Software, Formal analysis, Writing – original draft, Supervision, Validation. **José A. Zúñiga-Vicente:** Formal analysis, Validation, Writing – review & editing. All authors have read and agreed to the published version of the manuscript.

Declaration of Competing Interest

The authors declare that they have no known competing financial interests or personal relationships that could have appeared to influence the work reported in this paper.

Data Availability

The authors do not have permission to share data.

Acknowledgements

The authors would like to recognise the organisation SIGNUS ECOVALOR S.L.the support provided through the creation of the Aula Universidad Empresa SIGNUS, and to thank the APS office of Universidad Politécnica de Madrid for the project grant APS23.1001: "Nuevas vias de reciclaje y valorización de los NFU: posibilidades de aplicación en el sector de la construcción".

References

[1] P. Santos, T. Ribeiro, Thermal performance of double-pane lightweight steel framed walls with and without a reflective foil, Buildings 11 (7) (2021), https://doi.org/10.3390/buildings11070301.
[2] O.E. Ogunmakinde, T. Egbelakin, W. Sher, Contributions of the circular economy to the UN sustainable development goals through sustainable construction, Resour. Conserv. Recycl. 178 (2022), 106023, https://doi.org/10.1016/J.RESCONREC.2021.106023.
[3] R. Sikkema, D. Styles, R. Jonsson, B. Tobin, K.A. Byrne, A market inventory of construction wood for residential building in Europe – in the light of the Green Deal and new circular economy ambitions, Sustain. Cities Soc. 90 (2023), 104370, https://doi.org/10.1016/J.SCS.2022.104370.
[4] J.L. Gálvez-Martos, D. Styles, H. Schoenberger, B. Zeschmar-Lahl, Construction and demolition waste best management practice in Europe, Resour. Conserv. Recycl. 136 (2018) 166–178, https://doi.org/10.1016/J.RESCONREC.2018.04.016.
[5] T. Cerulli, C. Pistolesi, C. Maltese, D. Salvioni, Durability of traditional plasters with respect to blast furnace slag-based plaster, Cem. Concr. Res. 33 (9) (2003) 1375–1383, https://doi.org/10.1016/S0008-8846(03)00072-3.

[6] Y. Zhang, J. Yang, X. Cao, Effects of several retarders on setting time and strength of building gypsum, Constr. Build. Mater. 240 (2020), 117927, https://doi.org/10.1016/J.CONBUILDMAT.2019.117927.

[7] E.H. Elaiwi, et al., The influence of water-gypsum ratio on the properties of national gypsum (Joss) for various additives, Mater. Today Proc. (2023), https://doi.org/10.1016/J.MATPR.2023.01.081.

[8] A. Vidales-Barriguete, C. Piña-Ramírez, R. Serrano-Somolinos, M. del Río-Merino, E. Atanes-Sánchez, Behavior resulting from fire in plasterboard with plastic cable waste aggregates, J. Build. Eng. 40 (2021), 102293, https://doi.org/10.1016/j.jobe.2021.102293.

[9] D. Kaczorek, M. Basińska, H. Koczyk, Hygrothermal behaviour of a room with different occupancy scenarios, J. Build. Eng. 66 (2023), 105928, https://doi.org/10.1016/J.JOBE.2023.105928.

[10] M. Doleželová, J. Krejsová, L. Scheinherrová, M. Keppert, A. Vimmrová, Investigation of environmentally friendly gypsum based composites with improved water resistance, J. Clean. Prod. 370 (2022), 133278, https://doi.org/10.1016/J.JCLEPRO.2022.133278.

[11] L. Boccarusso, M. Durante, F. Iucolano, A. Langella, F.M.C. Minutolo, D. Mocerino, Recyclability process of standard and foamed gypsum, Procedia Manuf. 47 (2020) 743–748, https://doi.org/10.1016/J.PROMFG.2020.04.227.

[12] M.A. Pedreño-Rojas, J. Fořt, R. Černý, P. Rubio-de-Hita, Life cycle assessment of natural and recycled gypsum production in the Spanish context, J. Clean. Prod. 253 (2020), 120056, https://doi.org/10.1016/J.JCLEPRO.2020.120056.

[13] M. Del Río Merino, Aplicaciones del yeso y la escayola en la edificación. Nuevas aplicaciones, Inf. Constr. (2004) (Accessed 13 June 2022. [Online]. Available: ⟨https://www.researchgate.net/publication/26524588_Aplicaciones_del_yeso_y_la_escayola_en_la_edificacion_Nuevas_aplicaciones⟩).

[14] M. del Rio Merino, P. Villoria Sáez, I. Longobardi, J. Santa Cruz Astorqui, C. Porras-Amores, Redesigning lightweight gypsum with mixes of polystyrene waste from construction and demolition waste, J. Clean. Prod. 220 (2019) 144–151, https://doi.org/10.1016/J.JCLEPRO.2019.02.132.

[15] A. Bicer, F. Kar, Thermal and mechanical properties of gypsum plaster mixed with expanded polystyrene and tragacanth, Therm. Sci. Eng. Prog. 1 (2017) 59–65, https://doi.org/10.1016/J.TSEP.2017.02.008.

[16] S. Balti, A. Boudenne, L. Dammak, N. Hamdi, Mechanical and thermophysical characterization of gypsum composites reinforced by different wastes for green building applications, Constr. Build. Mater. 372 (2023), 130840, https://doi.org/10.1016/J.CONBUILDMAT.2023.130840.

[17] P.V. Sáez, M. del Río Merino, M. Sorrentino, C.P. Amores, J.S. Cruz Astorqui, C.V. Arrebola, Mechanical characterization of gypsum composites containing inert and insulation materials from construction and demolition waste and further application as a gypsum block, Materials 13 (1) (2020) 193, https://doi.org/10.3390/MA13010193.

[18] Z. Li, et al., Physical and mechanical properties of gypsum-based composites reinforced with basalt, glass, and PVA fibers, J. Build. Eng. 64 (2023), 105640, https://doi.org/10.1016/J.JOBE.2022.105640.

[19] F. Valentini, A. Pegoretti, End-of-life options of tyres. A review, Adv. Ind. Eng. Polym. Res. 5 (4) (2022) 203–213, https://doi.org/10.1016/J.AIEPR.2022.08.006.

[20] World Business Council for Sustainable Development, Managing End-of-Life Tires, 2008. [Online]. Available: ⟨www.wbcsd.org/web/tires⟩.

[21] F. Pacheco-Torgal, Y. Ding, S. Jalali, Properties and durability of concrete containing polymeric wastes (tyre rubber and polyethylene terephthalate bottles): an overview, Constr. Build. Mater. 30 (2012) 714–724, https://doi.org/10.1016/J.CONBUILDMAT.2011.11.047.

[22] A. Mohajerani, et al., Recycling waste rubber tyres in construction materials and associated environmental considerations: a review, Resour. Conserv. Recycl. 155 (2020), 104679, https://doi.org/10.1016/J.RESCONREC.2020.104679.

[23] A. Calabi-Floody, C. Mignolet-Garrido, G. Valdés-Vidal, Evaluation of the effects of textile fibre derived from end-of-life tyres (TFELT) on the rheological behaviour of asphalt binders, Constr. Build. Mater. 360 (2022), 129583, https://doi.org/10.1016/J.CONBUILDMAT.2022.129583.

[24] F. Parres, J.E. Crespo-Amorós, A. Nadal-Gisbert, Mechanical properties analysis of plaster reinforced with fiber and microfiber obtained from shredded tires, Constr. Build. Mater. 23 (10) (2009) 3182–3188, https://doi.org/10.1016/J.CONBUILDMAT.2009.06.040.

[25] A. Asadi Ardebili, P. Villoria Sáez, M. González Cortina, D.M. Tasán Cruz, Á. Rodríguez Sáiz, E. Atanes-Sánchez, Mechanical characterization of gypsum mortars with waste from the automotive sector, Constr. Build. Mater. 370 (2023), 130675, https://doi.org/10.1016/J.CONBUILDMAT.2023.130675.

[26] M.A. Pedreño-Rojas, J. De Brito, I. Flores-Colen, M.F.C. Pereira, P. Rubio-de-Hita, Influence of gypsum wastes on the workability of plasters: heating process and microstructural analysis, J. Build. Eng. 29 (2020), 101143, https://doi.org/10.1016/J.JOBE.2019.101143.

[27] S. Bouzit, et al., Investigation of thermo-acoustic and mechanical performance of gypsum-plaster and polyester fibers based materials for building envelope, Mater. Today Proc. 58 (2022) 1578–1581, https://doi.org/10.1016/J.MATPR.2022.03.560.

[28] Y. Kang, S.J. Chang, S. Kim, Hygrothermal behavior evaluation of walls improving heat and moisture performance on gypsum boards by adding porous materials, Energy Build. 165 (2018) 431–439, https://doi.org/10.1016/J.ENBUILD.2017.12.052.

[29] M. Álvarez, P. Santos, P. Lopes, D. Abrantes, D. Ferrández, Performance characterisation of a new plaster composite lightened with end-of-life tyres' recycled materials for false ceiling plates, Materials 15 (16) (2022) 5660, https://doi.org/10.3390/MA15165660.

[30] H.C. Wu, Y.M. Xia, X.Y. Hu, X. Liu, Improvement on mechanical strength and water absorption of gypsum modeling material with synthetic polymers, Ceram. Int. 40 (9) (2014) 14899–14906, https://doi.org/10.1016/J.CERAMINT.2014.06.085.

[31] Y. Zhao, et al., Fabrication of PMMA/phosphogypsum non-fired ceramic composites with improved mechanical and waterproof properties, J. Aust. Ceram. Soc. 57 (2021) 81–90, https://doi.org/10.1007/s41779-020-00510-z/Published.

[32] M. Álvarez, D. Ferrández, P. Guijarro-Miragaya, C. Morón, Characterization and under water action behaviour of a new plaster-based lightened composites for precast, Materials 16 (2) (2023) 872, https://doi.org/10.3390/MA16020872.

[33] M.Y. Durgun, Effect of wetting-drying cycles on gypsum plasters containing ground basaltic pumice and polypropylene fibers, J. Build. Eng. 32 (2020), 101801, https://doi.org/10.1016/J.JOBE.2020.101801.

[34] A. Vidales-Barriguete, E. Atanes-Sánchez, M. del Río-Merino, C. Piña-Ramírez, Analysis of the improved water-resistant properties of plaster compounds with the addition of plastic waste, Constr. Build. Mater. 230 (2020), 116956, https://doi.org/10.1016/J.CONBUILDMAT.2019.116956.

[35] D. Ferrández, A. Zaragoza, C. Morón, Material de construcción aislante aligerado, panel o placa prefabricado, proceso de elaboración de dicho material de construcción y de dicho panel o placa prefabricado, P202230251, 2022.

[36] R.V. Lozano-Díez, Ó. López-Zaldívar, S. Herrero-Del-cura, P.L. Mayor-Lobo, F. Hernández-Olivares, Mechanical behavior of plaster composites based on rubber particles from end-of-life tires reinforced with carbon fibers, Materials 14 (14) (2021) 3979, https://doi.org/10.3390/MA14143979.

[37] Z. Wang, H. Hu, J. Gong, Framework for modeling operational uncertainty to optimize offsite production scheduling of precast components, Autom. Constr. 86 (2018) 69–80, https://doi.org/10.1016/J.AUTCON.2017.10.026.

[38] Y. Dan, G. Liu, Y. Fu, Optimized flowshop scheduling for precast production considering process connection and blocking, Autom. Constr. 125 (2021), 103575, https://doi.org/10.1016/J.AUTCON.2021.103575.

[39] Z. Wang, H. Hu, J. Gong, Simulation based multiple disturbances evaluation in the precast supply chain for improved disturbance prevention, J. Clean. Prod. 177 (2018) 232–244, https://doi.org/10.1016/J.JCLEPRO.2017.12.188.

[40] A. Konczak, J. Paslawski, Decision support in production planning of precast concrete slabs based on simulation and learning from examples, Procedia Eng. 122 (2015) 81–87, https://doi.org/10.1016/J.PROENG.2015.10.010.

[41] M. del Rio Merino, C. Gómez Moreira, P. Villoria Sáez, Mechanical behavior of a gypsum material with additions of recycled waste from absorbent hygienic products, Constr. Build. Mater. 367 (2023), 130247, https://doi.org/10.1016/J.CONBUILDMAT.2022.130247.

[42] D. Ferrández, E. Yedra, I. Recalde-Esnoz, H. del Castillo, Reuse of end-of-life tires and their impact on the setting time of mortars: experimental study using a new measuring equipment, J. Build. Eng. 69 (2023), 106255, https://doi.org/10.1016/J.JOBE.2023.106255.

[43] J. Hidalgo-Crespo, C.M. Moreira, F.X. Jervis, M. Soto, J.L. Amaya, L. Banguera, Circular economy of expanded polystyrene container production: environmental benefits of household waste recycling considering renewable energies, Energy Rep. 8 (2022) 306–311, https://doi.org/10.1016/J.EGYR.2022.01.071.

[44] D. Landi, S. Gigli, M. Germani, M. Marconi, Investigating the feasibility of a reuse scenario for textile fibres recovered from end-of-life tyres, Waste Manag. 75 (2018) 187–204, https://doi.org/10.1016/J.WASMAN.2018.02.018.

[45] UNE-EN 13279-2:2014, Yesos de construcción y conglomerantes a base de yeso para la construcción. Parte 2: Métodos de ensayo. 2014.

[46] S. Balti, A. Boudenne, N. Hamdi, Characterization and optimization of eco-friendly gypsum materials using response surface methodology, J. Build. Eng. 69 (2023), 106219, https://doi.org/10.1016/J.JOBE.2023.106219.
[47] UNE-EN 1936:2007, Natural stone test methods – determination of real density and apparent density, and of total and open porosity, 2007.
[48] UNE-EN 14617-1, Agglomerated stone. Test methods. Part 1: identification of the apparent density and water absorption, 2013. [Online]. Available: ⟨www.aenor.es⟩.
[49] UNE-EN 520:2005+A1, Placas de yeso laminado. Definiciones, especificaciones y métodos de ensayo, 2010.
[50] M. del Río Merino, Elaboración y aplicaciones constructivas de paneles prefabricados de escayola aligerada y reforzada con fibras de vidrio E y otros aditivos, Universidad Politécnica de Madrid, Madrid, Spain, 1999, https://doi.org/10.20868/UPM.thesis.612.
[51] Ministry of Labour and Social Economy, National Institute of Safety and Health at Work. ⟨https://www.insst.es/⟩, (Accessed 23 April 2023).
[52] J. Heizer, B. Render, C. Munson, Operations Management: Sustainability and Supply Chain, 12th ed., PEARSON, Boston, USA, 2017.
[53] R. Siddique, T.R. Naik, Properties of concrete containing scrap-tire rubber – an overview, Waste Manag. 24 (6) (2004) 563–569, https://doi.org/10.1016/J.WASMAN.2004.01.006.
[54] A. San-Antonio-González, M.D.R. Merino, C.V. Arrebola, P. Villoria-Sáez, Lightweight material made with gypsum and EPS waste with enhanced mechanical strength, J. Mater. Civ. Eng. 28 (2) (2015), 04015101, https://doi.org/10.1061/(ASCE)MT.1943-5533.0001382.
[55] Ma. José Leiva Aguilera. Escayola aditivada con residuos de cáscara de arroz, Universidad Politécnica de Madrid, Madrid, Spain, 2017.
[56] M.I. Romero-Gómez, R.V. Silva, I. Flores-Colen, J. de Brito, Influence of polypropylene residues on the physico-mechanical and water-resistance properties of gypsum plasters, J. Clean. Prod. 371 (2022), 133674, https://doi.org/10.1016/J.JCLEPRO.2022.133674.
[57] J. Hao, G. Cheng, T. Hu, B. Guo, X. Li, Preparation of high-performance building gypsum by calcining FGD gypsum adding CaO as crystal modifier, Constr. Build. Mater. 306 (2021), 124910, https://doi.org/10.1016/J.CONBUILDMAT.2021.124910.
[58] Q. Wu, H. Ma, Q. Chen, B. Gu, S. Li, H. Zhu, Effect of silane modified styrene-acrylic emulsion on the waterproof properties of flue gas desulfurization gypsum, Constr. Build. Mater. 197 (2019) 506–512, https://doi.org/10.1016/J.CONBUILDMAT.2018.11.185.
[59] A. Zaragoza-Benzal, D. Ferrández, P. Santos, C. Morón, Recovery of end-of-life tyres and mineral wool waste: a case study with gypsum composite materials applying circular economy criteria, Materials 16 (243) (2023), https://doi.org/10.3390/MA16010243.
[60] R.M. Gonçalves, A. Martinho, J.P. Oliveira, Evaluating the potential use of recycled glass fibers for the development of gypsum-based composites, Constr. Build. Mater. 321 (2022), 126320, https://doi.org/10.1016/J.CONBUILDMAT.2022.126320.
[61] D. López Pedrajas, M. Carmona Franco, I. Garrido Sáenz, F.J. Ramos Mellado, J.F. Rodríguez Romero, A.M. Borreguero Simón, Polystyrene nanoparticles slurry as an additive for developing insulating and waterproof gypsum composites, Appl. Therm. Eng. 217 (2022), 119271, https://doi.org/10.1016/J.APPLTHERMALENG.2022.119271.
[62] X. Lu, H. He, Y. Wang, Y. Guo, X. Fei, Masses and size distributions of mechanically fragmented microplastics from LDPE and EPS under simulated landfill conditions, J. Hazard. Mater. 445 (2023), 130542, https://doi.org/10.1016/J.JHAZMAT.2022.130542.
[63] J. Fleith de Medeiros, T. Bisognin Garlet, J.L. Duarte Ribeiro, M. Nogueira Cortimiglia, Success factors for environmentally sustainable product innovation: an updated review, J. Clean. Prod. 345 (2022), 131039, https://doi.org/10.1016/J.JCLEPRO.2022.131039.
[64] N.H. Karim, N.S.F. Abdul Rahman, S.F.S. Syed Johari Shah, Empirical evidence on failure factors of warehouse productivity in Malaysian logistic service sector, Asian J. Shipp. Logist. 34 (2) (2018) 151–160, https://doi.org/10.1016/J.AJSL.2018.06.012.
[65] C. Chen, X. Li, W. Yao, Z. Wang, H. Zhu, Analysis of the impact of construction robots on workers' health, Build. Environ. 225 (2022), 109595, https://doi.org/10.1016/J.BUILDENV.2022.109595.
[66] O. Oloruntobi, K. Mokhtar, N. Mohd Rozar, A. Gohari, S. Asif, L.F. Chuah, Effective technologies and practices for reducing pollution in warehouses – a review, Clean. Eng. Technol. 13 (2023), 100622, https://doi.org/10.1016/J.CLET.2023.100622.
[67] Z. Dong, Y. Tan, L. Wang, J. Zheng, S. Hu, Green supply chain management and clean technology innovation: an empirical analysis of multinational enterprises in China, J. Clean. Prod. 310 (2021), 127377, https://doi.org/10.1016/J.JCLEPRO.2021.127377.
[68] S. Sun, Q. Wu, X. Tian, How does sharing economy advance cleaner production? Evidence from the product life cycle design perspective, Environ. Impact Assess. Rev. 99 (2023), 107016, https://doi.org/10.1016/J.EIAR.2022.107016.
[69] L. Lin, J. Xu, J. Yuan, Y. Yu, Compressive strength and elastic modulus of RBAC: an analysis of existing data and an artificial intelligence based prediction, Case Stud. Constr. Mater. 18 (2023), e02184, https://doi.org/10.1016/j.cscm.2023.e02184.
[70] Y. Yu, X. Zhao, T. Xie, X. Wang, Eco-, economic- and mechanical-efficiencies of using precast rejects as coarse aggregates in self-compacting concrete, Case Stud. Constr. Mater. 17 (2022), https://doi.org/10.1016/j.cscm.2022.e01591.
[71] M. Živicnjak, K. Rogic, I. Bajor, Case-study analysis of warehouse process optimization, Transp. Res. Procedia 64 (C) (2022) 215–223, https://doi.org/10.1016/J.TRPRO.2022.09.026.

3.4. Study of the hygroscopic properties of environmentally friendly lightened composites through waste recovery

Contents lists available at ScienceDirect

Construction and Building Materials

journal homepage: www.elsevier.com/locate/conbuildmat

Study of the hygroscopic properties of environmentally friendly lightened composites through waste recovery

Alicia Zaragoza-Benzal [a,*], Daniel Ferrández [a], Evangelina Atanes-Sánchez [b], Pablo Saíz [c]

[a] Universidad Politécnica de Madrid, Departamento de Tecnología de la Edificación, 28040 Madrid, Spain
[b] Universidad Politécnica de Madrid, Departamento de Ingeniería Mecánica, Química y Diseño Industrial, 28012 Madrid, Spain
[c] Universidad Rey Juan Carlos, Departamento de Economía Financiera, Contabilidad e Idioma Moderno, Paseo de los Artilleros, s/n, 28032 Madrid, Spain

ARTICLE INFO

Keywords:
Lightweight composite
Water resistance
Expanded polystyrene (EPS) waste
End-of-life tyres
Circular economy

ABSTRACT

Gypsum-plaster is becoming an ideal binder in the valorisation and recovery of waste for designing more sustainable composites. Nevetheless, the main limitation of plaster lies in its susceptibility to the action of water. In this research, a complete study of the hygroscopic properties of a new material has been carried out, in which plaster material has been partially substituted in mass by dissolved expanded polystyrene waste in percentages of 8.8% to 26.5%. Additionally, fibres from end-of-life tyres have been incorporated at 1.2% by mass to improve the strength and durability of the compounds, achieving a total reduction of up to 28% of the original raw materials. The experimental campaign delves into the water performance of this new plaster composites through mercury porosimetry tests, water absorption by capillarity, total water absorption, water vapour permeability, Karsten Tube penetration, water-stove cycles, as well as the analysis of images obtained by scanning electron microscopy. The main results obtained show a reduction of 97.8% in surface water absorption, as well as a decrease of up to 17.44% in water vapour permeability compared to traditional plaster. Moreover, the developed materials exhibit good mechanical behaviour after undergoing several accelerated ageing cycles. This work highlights the potential of the new plaster composites designed to produce a more sustainable alternative to commercial prefabricated boards and panels, especially suitable for use in interior rooms where high resistance to the action of water is required.

1. Introduction

Industrialised construction has emerged in response to the challenges facing the building sector in terms of productivity and sustainability [1,2]. The vulnerability of the sector to resource scarcity, lack of skilled labour and the energy crisis make industrialisation and prefabrication the cornerstones of the future of construction [3]. However, the implementation of this production system requires the development of new materials with high technical performance, which in turn respond to the demands of sustainable development set by organisations and governments worldwide [4–6].

Plaster is one of the binders that requires the least amount of energy for its production and is currently one of the construction materials that releases the least amount of greenhouse gas emissions into the atmosphere during its production process [7]. This aspect, together with its great versatility and workability, as well as its low specific weight, and its good insulating properties, both thermal and acoustic [8], have led to this material being widely used in construction. Plaster is positioned as a very interesting material from the point of view of industrialised construction, making it possible to produce prefabricated elements and systems with reduced delivery times and minimise costs thanks to the speed of its placement on site, and the ease of its transport and assembly [9].

Nevertheless, the main limitation of the use of gypsum is its behaviour in contact with water. In the presence of moisture, the plaster material degrades rapidly due to the weakening of the cohesive forces between the gypsum crystals, resulting in a large loss of mechanical strength [10]. In addition, the accumulation of moisture can promote the appearance of efflorescence or fungi on its surface, being detrimental not only for the material itself [11], but also for people's health [12]. In this sense, several studies have been carried out to increase the water resistance of plaster, with two main procedures being highlighted:

* Corresponding author.
E-mail addresses: alicia.zaragoza@upm.es (A. Zaragoza-Benzal), daniel.fvega@upm.es (D. Ferrández), evangelina.atanes@upm.es (E. Atanes-Sánchez), pablo.saiz@urjc.es (P. Saíz).

https://doi.org/10.1016/j.conbuildmat.2023.133219
Received 21 June 2023; Received in revised form 28 August 2023; Accepted 1 September 2023

creating an impermeable layer on the hardened plaster material or modifying the internal structure of the material by incorporating hydrophobic additions. Surface treatments, such as the application of epoxy resins [13], methyl methacrylate [11] or latex [14] on the hardened plaster, although effective in the short term, involve longer production processes and require continuous maintenance to prevent the loss of its waterproof properties. On the other hand, more durable and effective results have been achieved with the incorporation of additions to the fresh plaster mix. This is the case of cementitious additions [15], as silicate clinker [7], silica fume [16] and slag [17]; in these cases, although there were increases in the water resistance of the plaster, a significant increase in the specific weight of the resulting material was also observed [11], as well as an increase in cracks and fissures in the plaster, reducing its mechanical performance [7].

Other researchers have studied the incorporation of additives such as superplasticisers [18], which made the final product considerably expensive. On the other hand, López Pedrajas et al. managed to improve the impermeability of the plaster by introducing a dispersion of synthesised polystyrene nanoparticles [19]. As in the research by Wu et al., these polymer emulsions manage to create an impermeable film around the gypsum crystals, ensuring a homogeneous distribution throughout the plaster mix in the fresh state [20]. However, it was observed that an excess of addition led to a decrease in mechanical strength due to a reduction in the compactness of the composites produced.

In all the aforementioned studies, the negative effects of water on plaster have been reduced to a certain extent by incorporating different raw materials. However, several studies have shown the need to introduce manufacturing methods and processes under circular economy criteria if we want to move towards more sustainable development and make responsible use of resources [21]. For this reason, some research has currently been carried out in order to study the reintroduction of waste in the manufacturing process of plasters with waterproofing properties. This is the case of Vidales-Barriguete et al. who, by introducing plastic cable waste, managed to improve the resistance of the plaster composites to moisture [22], as well as reducing the porosity of the material and slightly increasing its bulk density. Romero-Gómez et al. studied the good waterproofing properties of polypropylene waste as a partial replacement in gypsum composites, limiting the amount of waste incorporated to 10%, as the workability of the paste decreased with higher proportions [23]. It was observed that with 2.5% of polypropylene residues, an increase in density was produced, which improved the compressive strength of the composites by 1.2 MPa with respect to the reference, however, the flexural strength decreased by up to 35%. Other types of additives, such as organic additives (bio-fillers), which have a low environmental impact, have also been studied in plaster composites. Specifically, the scallop shell waste reached densities of around 1530 kg/m^3, as the small size of the incorporated particles managed to fill the existing pores in the plaster matrix. In addition, there was a significant improvement in mechanical strength due to the high concentrations of calcium carbonate present in the scallop shells [24].

Regarding waste recovery, one of the research lines that is currently generating most interest is the reuse and revaluation of plastic waste due to its slow degradation process and strong environmental impact [25]. In recent years, EPS waste has been increasing due to its growing use in packaging and as thermal insulation in buildings because of its good insulating characteristics, low density and low cost [26]. In 2020, EPS production in the EU reached 1.55 Mt, and this figure is expected to double by 2030 [27]. The low density of EPS waste means that, compared to other plastics, it occupies large volumes difficult to manage in landfills [28]. This waste can be recycled mechanically, which requires a high purity of the waste that is complicated to achieve [29]. Another method of utilising EPS waste is energy recuperation through incineration, which releases large amounts of CO_2 and other environmentally harmful chemical compounds into the atmosphere [28]. However, the system that is currently achieving the best results is chemical recycling [27].

Numerous studies have shown that additions of EPS residues in plaster reduce the specific weight of the composites, although this characteristic is associated with a weakening of the mechanical strength of the material [30]. This decrease in mechanical properties is caused by the poor bonding between the gypsum crystals and the EPS particles, generating discontinuities and preferential breakage points in the plaster matrix [31]. Nevertheless, the behaviour of gypsum plasters towards water with the incorporation of EPS waste from construction and demolition waste (CDW) has been barely studied.

As with EPS waste, end-of-life tyres also require large landfill spaces for storage. By 2030, it is expected that more than 1.2 billion end-of-life tyres will be generated annually [32], causing serious environmental damage. This is why many studies are focusing on developing ways to reincorporate these wastes into the production process of other materials, thus creating circular systems (close-loop scenarios) of waste reuse. Currently, three main by-products are obtained from ELT recycling: rubber (47%), steel fibres (12%) and textile fibres (10%) [33]. Recycled rubber and steel have already established reuse processes in the industry [34], however, today there is still no clear application for textile fibres from ELT. Some researchers have studied the incorporation of these fibres in concretes, geopolymers and bituminous materials [33] with the intention of reducing cracking during setting and increasing the ductility of the materials. They are also used in the production of aerogels, as these fibres are noted for their low thermal conductivity [35].

The main objective of this research is to develop highly water-resistant lightweight plaster composites by incorporating EPS waste in dissolution, and with good physico-mechanical properties through the addition of ELT textile fibres. Thus, unlike other research reviewed in the literature where EPS waste was introduced as solid particles, in this research the waste is incorporated in a liquid state during the mixing process, improving its integration and the homogeneity of the plaster matrix. In this way, it is expected that the hydrophobic properties of EPS, along with the ELT textile fibres properties, will result in a lightweight, strong and durable material.

With the new developed material, the field of use for plaster composites is significantly extended in the construction sector, allowing the production of lightweight prefabricated products that can be used in environments with a high degree of humidity or in direct contact with water. This research is therefore in line with Sustainable Development Goals 11 and 12 of the 2030 Agenda [6], contributing to the reduction of raw material consumption and the recirculation of construction waste. It should be noted that the original nature of this research work has allowed the developed material to be patented at the Spanish Patent and Trademark Office (OEPM), with registration number P202230251 [36].

2. Materials and methods

2.1. Materials

The following materials were used in the production of the composites developed in this research: E-35 plaster, EPS waste, universal solvent, ELT textile fibres and water.

2.1.1. Binder

Plaster E-35, type A according to UNE-EN 13279-1:2009 [37], supplied by Placo Saint-Gobain (Madrid, Spain), was used as a binder. This material is characterised by a high purity index (greater than92%) and a fine granulometry, with a particle size of 0–2 mm. According to the data provided by the manufacturer, this type of plaster has the following properties: water vapour diffusion resistance factor (μ) 6; thermal conductivity coefficient 0.3 W/mK; flexural strength greater than 3.5 N/mm^2 and pH greater than 6 [38].

2.1.2. Expanded polystyrene (EPS) waste

EPS is an insulating material commonly used in buildings, which is obtained from the polymerisation and subsequent expansion of styrene

monomers. It is a low density, rigid and economical material, which makes it ideal for the execution of External Thermal Insulation Composite System (ETICS) [39]. The EPS waste used in this research comes from façade rehabilitation works using ETICS located in the Community of Madrid. The characteristics of this type of insulation are specified below: density between 28 and 30 kg/m^3, thermal conductivity coefficient 0.031 W/mK and water vapour diffusion resistance factor (μ) between 20 and 100 [40].

2.1.3. Universal solvent

For the dissolution of the EPS waste, Nazza universal solvent (Seville, Spain) was used. This product is a colourless liquid, formed by the combination of different chemical agents from volatile hydrocarbons, which have a strong dissolving power on organic compounds. The solvent used is composed of toluene, xylene, n-butyl acetate, ethyl acetate, ethylbenzene, acetone, propan-2-one and propanone. The main properties provided by the manufacturer are as follows: vapour pressure 85.5 mmHg at 20 °C and density at 20 °C (ASTM D 1298/4052) 812 ± 20 kg/m^3 [41].

2.1.4. Textile fibres from End-of-Life tyres (ELT)

From the recycling of ELT, among other by-products, textile fibres are obtained, which are mainly composed of synthetic fibres such as rayon, nylon and polyester [42]. These fibres are considered a special waste (EWC code 19.12.08) [33] and therefore must be stored or burned, both scenarios being harmful to the environment as the accumulation of these wastes is estimated to reach 320 kilotonnes per year just in Europe [43]. Table 1 lists the main characteristics of textile fibres from ELT according to the literature.

Fig. 1 (a) shows the textile fibres used in this study, where a certain amount of adhered rubber remains can be observed. Fig. 1 (b) shows a scanning electron microscopy of these fibres using a Jeol JSM-820 microscope operating at 20 kV, equipped with Oxford EDX analysis.

2.1.5. Water

In the kneading process, impurity-free drinking water from the Canal de Isabel II of the Community of Madrid was employed, which has been shown to be suitable for use in this type of research in previous studies [44]. Its main characteristics include its medium hardness with 25 mg/l of $CaCO_3$ and its pH between 7 and 8.5.

2.2. Preparation of samples

The sample preparation process is divided into two stages. First, the EPS residues are dissolved with universal solvent. This stage is the main difference with other studies where solid EPS waste is introduced into plaster composites [45,46], as this procedure allows obtaining much more homogeneous mixtures and a cohesive matrix. For this process, the solvent is poured into a container in which the EPS waste is progressively introduced. In this way, thanks to the low polar chemical nature of both materials, the styrene polymer that forms the EPS (Fig. 2 (a)) is broken down into monomers by the action of the solvent, resulting in a viscous liquid (Fig. 2 (b)), with a density of 660 kg/m^3.

In the second stage, the plaster and water are mixed according to standard UNE-EN 13279-2: 2014 [47], which specifies the following procedure: the plaster powder is sprinkled on the water for 30 s, it is left to stand for one minute, then manual mixing is started with planetary movements for another 30 s, it is left to stand again for 30 s, and finally, it is mixed again manually for 30 s. The incorporation of the EPS waste solution prepared previously is carried out prior to the last mixing, when the plaster/water mixture is still in a liquid state. On the other hand, in those mixes with the incorporation of ELT textile fibres, these are previously dispersed in the plaster powder before starting the mixing process to ensure the adequate dispersion of the fibres. Once the mixing process is finished, the mixtures are poured into the corresponding moulds, being demoulded once the material has set, storing the specimens in a laboratory environment with a temperature of 23 ± 2 °C and 50 ± 5 % relative humidity for 7 days, to subsequently carry out the tests.

Table 1
ELT textile fibres main technical characteristics [50,52,54,65].

Thermal conductivity coefficient	0.0548–0.0632 W/mK
Rubber residue content	5–20%
Length	20–40 mm
Average diameter	22.5 μm
Average density	175 kg/m^3

The water/plaster ratio was determined using the shaking table method described in UNE-EN 13279–2: 2014 [47]. This standard specifies that the paste must reach a diameter of 165 ± 5 mm after the test, obtaining a water/plaster ratio of 0.7 by mass. Maintaining this ratio for all the proposed dosages, the amount of water and plaster was gradually reduced, replacing it progressively by mass with the EPS solution. In this way, the aim is to obtain maximum savings in raw materials, with the greatest possible incorporation of waste. Likewise, another series of composites was produced with the addition of ELT textile fibres and the dissolution of EPS waste, also carrying out the corresponding proportional reduction of raw materials. The purpose is to study the effects of this type of fibres on the composites with the additions of dissolved EPS. The dosages are shown in Table 2, where the nomenclature used is E0.7-X-N, where E0.7 refers to the water/stuff ratio obtained, X refers to the amount of EPS dissolution by mass added and finally, if applicable, N indicates the incorporation of textile fibres.

Taking as a starting point the reference sample E0.7 shown in Table 2, the amount of plaster powder and water has been progressively reduced in each of the mixes. This replacement of the binder with recycled materials generates a saving of the original raw materials in the production of the plaster composites of up to 27.7% in the E0.7-450-N dosage. In this way, the production of eco-friendly gypsum based-composites for use in buildings is being promoted, contributing to the efficient use of resources in construction and the recovery of waste in line with the objectives set by The European Green Deal [48].

2.3. Experimental programme

With an original and novel character, this work analyses the behaviour of a new plaster composite with an improved response to the action of water. Fig. 3 shows a schematic and synthesised representation of the experimental programme carried out in this research.

2.3.1. Mercury porosimetry

Mercury porosimetry is carried out to be able to relate the water behaviour and the internal porous structure of the composites. The test consists of subjecting cylindrical specimens, 10 mm in diameter and 10 mm in height, to progressively increasing pressures of mercury, until reaching a maximum pressure of 227 MPa, in a constant vacuum environment of 50 μmHg for five minutes and room temperature. The data obtained at the end of the test are the following: total pore volume, volume mean pore diameter, porosity percentage of the samples, bulk density and skeleton density. The equipment used for this test was Autopore IV 9500 from Micromeritics Instrument Corporation.

2.3.2. Capillary water absorption

The purpose of this test is to determine the maximum height that water is capable of reaching in samples of 40 × 40 × 160 mm due to the effect of capillary absorption of the material [49]. For this purpose, the specifications of the RILEM RC 25-PEM standard were followed [50], which indicates that the samples should be placed vertically in a container with water on a grid that avoids direct contact with the bottom of the container. At the start of the test, the water level should reach a height of 10 mm ± 1 mm above the base of the specimens (Fig. 4). Then,

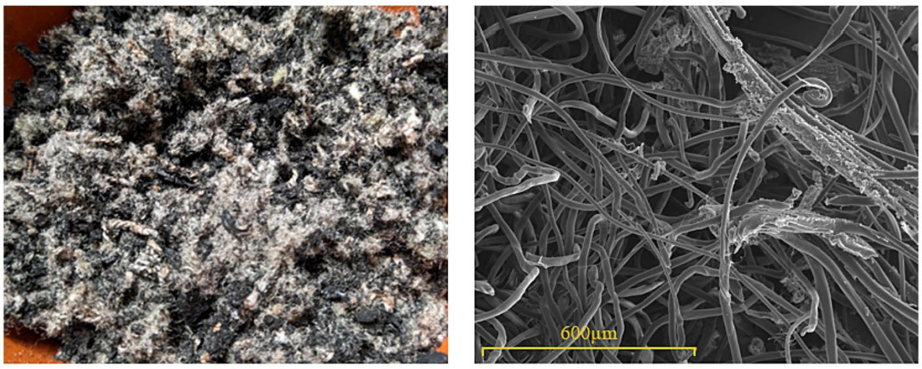

Fig. 1. (a) ELT textile fibres; (b)Scanning electron microscopy of ELT textile fibres, magnification x150.

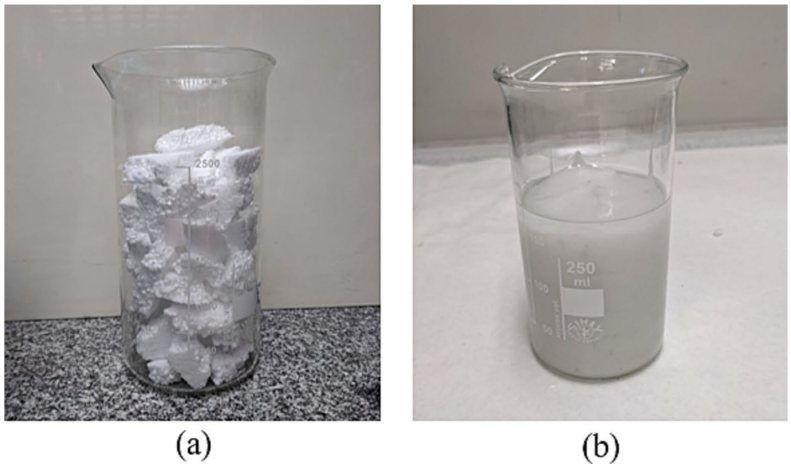

Fig. 2. (a) Solid EPS waste; (b) Dissolved EPS.

Table 2
Dosages used in this study.

Sample	Plaster (g)	Water (g)	Dissolved EPS (g)	Textile fibres (g)	Raw material consumption savings (%)*
E0.7 (Ref.)	700	1000	_	_	0
E0.7–150	911	639	150	_	8.8
E0.7–300	824	576	300	_	17.7
E0.7–450	735	515	450	_	26.5
E0.7-N	988	692	_	20	1.2
E0.7–150-N	900	630	150	20	10
E0.7–300-N	812	568	300	20	18.8
E0.7–450-N	724	506	450	20	27.7

*Savings referred to the water and plaster used in the production of the plaster paste for the reference dosage.

the level reached by the water due to capillarity is recorded every minute for a total of 10 min, expressing the results in millimetres per minute (mm/min).

2.3.3. Total water absorption

The total water absorption of the composites is determined by the percentage increase in mass of the samples after a given time, according to the indications of the UNE-EN 520 standard [51]. The 300 × 300 × 15 mm samples are weighed and then placed in a container with water, the level of which must be between 25 and 35 mm above the surface of the samples. The samples must be placed on a grid to avoid contact with the bottom of the container. After 2 h ± 2 min, the specimens are removed from the container, the excess water removed and the weights noted again. The total water absorption coefficient is expressed as a percentage using equation (1):

$$\Delta\ mass\ (\%) = \frac{w_{2h} - w_0}{w_0} \cdot 100 \quad (1)$$

where, w_{2h} is the weight of the sample after two hours immersion, and w_0 is the initial weight of the sample.

2.3.4. Water vapour permeability

Following the UNE-EN 12,572 standard [52], the mass of water vapour that is capable of passing through the test samples per unit area and time under isothermal conditions is determined. For this purpose, a saturated aqueous solution of potassium nitrate is prepared and poured into the test container, thus ensuring a relative humidity of around 94%

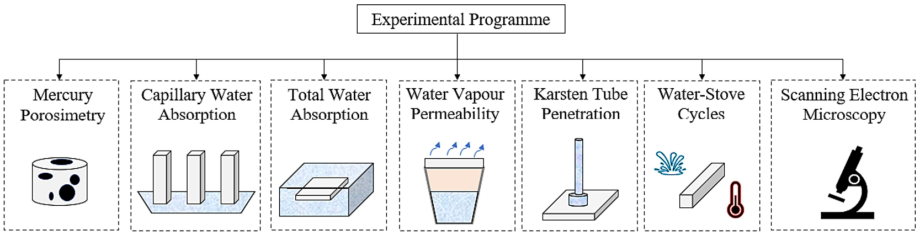

Fig. 3. Schematic representation of the different stages included in the experimental programme.

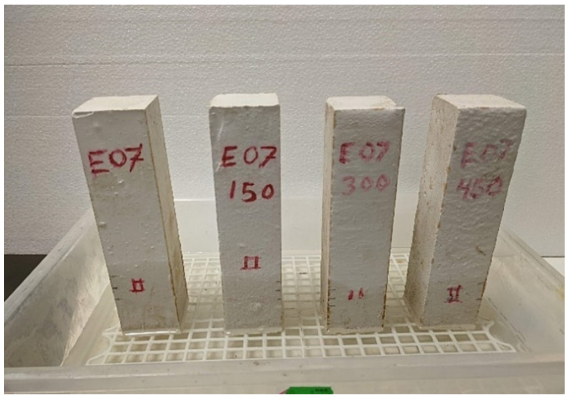

Fig. 4. Samples during the capillary water absorption test.

inside the sealed container. The 1,5 ± 0,5 cm thick disc-shaped samples are then hermetically fixed to the test vessel. The container-sample ensemble is kept at a constant temperature of 23 ± 5 °C and weighed weekly for 8 weeks. Once the weights have been obtained, and by applying equations (2), (3), (4) and (5), the water vapour permeability of the compounds is obtained.

$$P = PR \cdot e \tag{2}$$

$$PR = \mathrm{WVT}/\cdot p \tag{3}$$

$$\Delta p = S(R1 - R2) \tag{4}$$

$$WVT = \Delta m/(t \cdot A) \tag{5}$$

Table 3
Description of the variables in equations (2), (3), (4) and (5).

Variable	Description	Units
P	Water vapour permeability	g/(m·h·mmHg)
e	Thickness of specimens	m
PR	Water vapour permeance	g/(m^2·h·mmHg)
WVT	Water vapour transmission rate	g/(m^2·h)
Δp	Water vapour pressure difference to partial vapour pressure during the test	mmHg
S	Saturation pressure of water vapour at test temperature*	mmHg
$R1$	Relative humidity of the side with the highest water vapour pressure during the test (94%)	%
$R2$	Relative humidity of the side with the lowest vapour pressure (50%)	%
Δm	Mass variation	g
t	Time between measurements	h
A	Area of test sample	m^2

*Note: Average temperature 21 °C and saturation pressure 18,663 mmHg.

Table 3 shows the description corresponding to each of the variables in equations (2), (3), (4) and (5).

2.3.5. *Karsten tube penetration test*

The surface permeability was obtained by means of the Karsten tube test according to the RILEM method [53]. This test allows to determine the amount of water absorbed per unit of time and surface in direct contact with the water. The Karsten tube is fixed hermetically to the surface to be tested and filled with water to create a 10 cm column (Fig. 5). The water level is then recorded by the graduating tube at 5, 10, 15, 15, 20, 30 and 60 min of testing and the results are expressed in mm of water absorbed per minute. Although this test is more suitable for materials used outdoors, it is considered interesting to carry it out in order to know the waterproof potential of the plaster composites developed.

2.3.6. *Water-stove cycles*

This non-standardised test, developed by Del Río Merino in his doctoral thesis [54], aims to determine the durability of plaster composites by studying the mass loss of the samples, as well as the variation

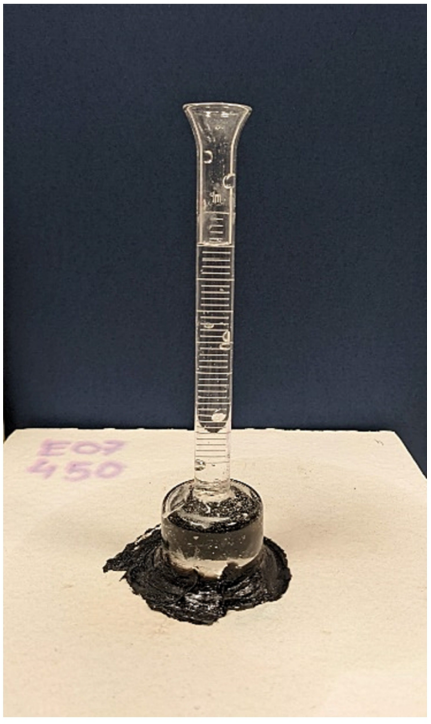

Fig. 5. Karsten Tube Penetration Test.

in their physical and mechanical properties after subjecting the material to water-stove cycles. Standard RILEM samples measuring 40 × 40 × 160 mm are used and weighed at the start of the test. The first cycle begins by placing the samples in a container with water, completely submerged and separated from the bottom of the container by a grid, for two days. Subsequently, the specimens are placed in an oven for a further two days at a temperature of 60 °C and a relative humidity of 50 %. This water-stove cycle has to be carried out once more. Finally, the final weight of the samples, the Shore C surface hardness, the modulus of elasticity by ultrasound (MOE_{US}) and the flexural and compressive strength of the samples subjected to the cycles are determined. Likewise, to have a reference with which to compare the results, the physical and mechanical characterisation tests are also carried out on a second series of samples, from the same mix and without undergoing the accelerated ageing cycles.

2.3.7. Statistical analysis of the results

The statistical analysis was conducted on the results of the capillary water absorption tests, total water absorption and the results of the physical–mechanical tests of the samples subjected to water-stove cycles. Considering three values for each of the properties, the factors and levels for the Analysis of Variance (ANOVA) included in Table 4 have been considered.

A multiple range test was also performed to analyse the existence or not of significant differences between the different levels analysed for each factor. Finally, the diagnosis of the model was checked to ensure compliance with the requirements of independence, normality and homoscedasticity of the residuals, thus ensuring a robust design of the experiments carried out.

2.3.8. Scanning electron microscopy (SEM)

The microscopic morphology of the samples was analysed by scanning electron microscopy using a Jeol JSM-820 microscope operating at 20 kV and equipped with Oxford EDX analysis. All fragments analysed were obtained ensuring that no surface disturbance occurred. To ensure adequate conductivity of the electron beam, a thin layer of gold was applied to the surface of the samples using a Cressington 108 metalliser.

3. Results and discussion

In this section, the results of the tests proposed in the experimental programme are presented, as well as their analysis and discussion.

3.1. Mercury porosimetry

Table 5 and Figs. 6 and 7 shows the results obtained from the mercury porosimetry test of all the compounds developed in this study.

As can be seen in Table 5, the total pore volume of the samples is directly proportional to the amount of dissolved EPS incorporated. In the case of the plaster with the addition of ELT textile fibres (E0.7-N), the total pore volume is slightly reduced with respect to the traditional plaster (E0.7), so that, in general terms, the composites containing both dissolved EPS and textile fibres have a smaller pore volume than the plaster containing only EPS. These results of the total pore volume are closely related to the percentage porosity of the samples, being the composites with the addition of fibres and dissolved EPS significantly less porous than the composites containing only EPS.

On the other hand, the composites with a higher amount of dissolved EPS in their composition obtained the lowest bulk density. The textile fibres generate an increase in the bulk density of the lightened plaster composites, although this decreases as the amount of dissolved EPS in the mixtures increases. Similarly, the lowest skeleton density occurs in the sample with the highest proportion of dissolved EPS (E0.7-450), with the textile fibres producing an increase in this density. However, all the skeleton densities of the composites with additions are higher than that of the reference plaster.

Table 4
Factors and levels used for the analysis of variance (ANOVA).

Factors	Levels	Nomenclature
Dosage	EPS dissolution in the samples	0 – 150 – 300 – 450
Fibers	No Fiber or With ELT Fiber	NF / WF

According to the results obtained, more than 90% of the pores of the developed composites can be considered macropores (Ø greater than 50 nm) according to the IUPAC standard [55]. It can be seen that the pore size increases as the amount of EPS dissolved in the samples increases, while the incorporation of ELT textile fibres reduces these pore sizes significantly.

As can be seen in Fig. 6 (a), overall, as the amount of EPS solution in the samples increases, the accumulated pore volume rises, being higher in sample E0.7–450. The steep slopes of the curves corresponding to samples E0.7–300 and E0.7–450 show a very narrow pore distribution, with a large amount of pore volume accumulating in the larger diameters present in the samples. However, sample E0.7–150 does not seem to follow this trend, since it presents a total pore volume even smaller than the reference. As for the samples incorporating textile fibres (Fig. 6 (b)), it can be observed that all of them show a similar pore volume, close to the reference plaster (E0.7), although sample E0.7–300-N shows a slight increase in volume with respect to the other samples with fibres.

On the other hand, Fig. 7 gives an overview of the internal microstructure of each material analysed in this research through differential pore volume distribution analysis.

As can be seen in Fig. 7, the composites incorporating dissolved EPS present a greater amount of large pores in their structure as the addition increases in the mixtures, being in this type of pores where most of the total pore volume is accumulated. In addition, it is observed that in sample E0.7–450 there is a significant increase in mesopores, with diameters of less than 50 nm. However, the samples with textile fibres have a larger number of mesopores than the composites that only incorporate the EPS solution, with a large part of the pore volume accumulating in the smaller diameters. These mesopores even increase proportionally as the amount of dissolved EPS increases. This effect can also be seen in Table 5, where the pore diameters of the samples with textile fibres decrease with respect to their counterparts without fibres.

3.2. Capillary water absorption

Table 6 shows the average value obtained for the capillary water absorption of each of the compounds included in this research.

For the statistical analysis of this test, the mean value of three samples of each type of plaster was used, as shown in Table 7. Furthermore, after performing the ANOVA on the data, a p-value of 0.000 was obtained for the Dosage factor and a p-value of 0.1247 for the Fibers factor, the latter being non-significant ($\alpha > 0.05$). Table 7 below shows the results obtained for the multiple range test to complement the discussion of the results.

The results obtained from the capillary water absorption test show how the incorporation of the EPS solution in the plaster composites manages to reduce the level reached by the water in the test samples after the test. Although it is true that there are no statistically significant differences between the composites with the three additions of EPS in solution, with the substitution of 450 g in mass of plaster by the dissolved EPS, the capillary water absorption was reduced by up to 28.9% with respect to the traditional plaster composites without EPS. These results agree with other studies where plastic residues have been incorporated, which limit the water absorption of the plaster [22].

On the other hand, the addition of textile fibres in the E0.7-N composite produced a 17.78% increase in water absorption. This effect may be due to the higher amount of small pore size (less than50 nm) in the plaster with textile fibres, observed in the mercury porosimetry test.

Table 5
Results obtained from mercury porosimetry of plaster composites.

Sample	Pore volume (cm^3/g)	Bulk density (g/cm^3)	Skeletal density (g/cm^3)	Porosity (%)	Pore size (nm) 0–10% Pore volume	10–50% Pore volume	50–90% Pore volume
E0.7	0.5007	0.8898	1.6061	44,5970	[36145–3613]	[3613–2685]	[2685–673]
E0.7–150	0.4491	1.0048	1.8325	45.1667	[36154–6032]	[6032–3706]	[3706–1046]
E0.7–300	0.6180	0.8731	1.8981	54.0031	[36143–7808]	[7808–5916]	[5916–3173]
E0.7–450	0.6991	0.7926	1.7778	55.4175	[36143–11306]	[11306–7808]	[7808–4770]
E0.7-N	0.4959	1.0676	2.2685	52.9392	[36147–3219]	[3219–2349]	[2349–673]
E0.7–150-N	0.5021	0.9867	1.9576	49.5977	[36147–4197]	[4197–3013]	[3013–1302]
E0.7–300-N	0.5238	0.9253	1.7957	48.4703	[36146–7561]	[7561–4675]	[4675–2817]
E0.7–450-N	0.5072	0.9485	1.8297	48.1598	[36146–9055]	[9055–6149]	[6149–3136]

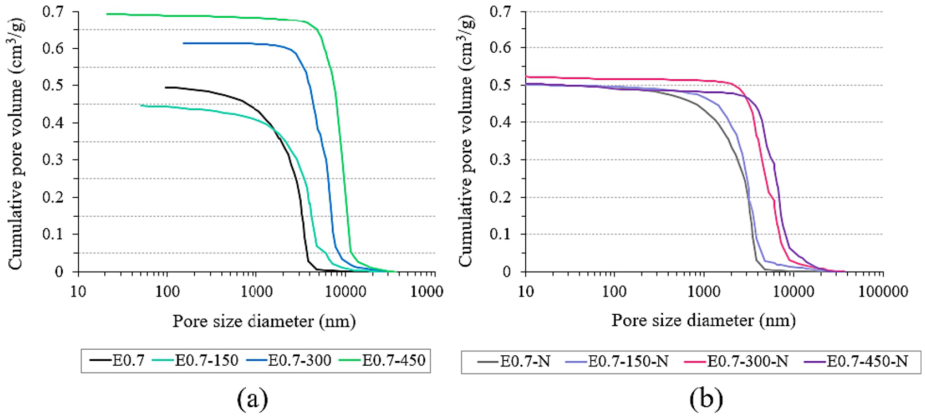

Fig. 6. Cumulative pore size distribution: (a) Samples E0.7, E0.7–150, E0.7–300 and E0.7–450; (b) Samples E0.7-N, E0.7–150-N, E0.7–300-N and E0.7–450-N.

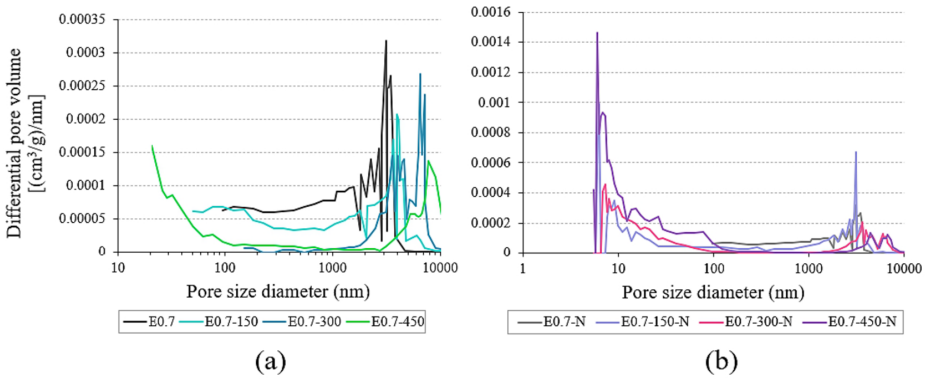

Fig. 7. Differential pore size distribution: (a) Samples E0.7, E0.7–150, E0.7–300 and E0.7–450; (b) Samples E0.7-N, E0.7–150-N, E0.7–300-N and E0.7–450-N.

Table 6
Capillary water absorption test results.

Sample	E0.7	E0.7–150	E0.7–300	E0.7–450	E0.7-N	E0.7–150-N	E0.7–300-N	E0.7–450-N
Average water uptake (mm/min)	4.5	3.6	3.2	3.2	5.3	3.5	3.6	3.3

These small pores, as indicated by Jurin's Law, cause the height reached by a fluid to be greater the smaller the radius of the capillary conduit, as long as there is interconnection between them [49]. The increase in water absorption produced by the addition of the fibres is counteracted when the EPS solution is added to the mixtures, again obtaining values similar to those of the plaster composites without ELT textile fibres. This effect suggests the water-repellent potential of plaster composites with EPS incorporation in solution, even in those composites where recycled raw materials have been added that promote the hygroscopicity of the original material [56].

Table 7
Multiple Range Test for capillary water absorption.

Factor	Levels	LS Mean	LS Sigma	Homogeneus Group
Dossage	450	32.50	1.2971	X
	300	34.00		X
	150	35.50		X
	0	49.16		X
Fibers	NF	36.75	0.9172	X
	WF	38.83		X

3.3. Total water absorption

Table 8 shows the results of the total water absorption test of the developed plaster composites.

The statistical analysis of the results obtained for total water absorption, shown in Table 9, was carried out using the mean of three compounds of each type. After ANOVA of the data included in the experiment, a p-value of 0.000 was obtained for the Dosage factor and a p-value of 0.6866 for the Fibers factor, the latter being non-significant (α greater than 0.05). Similarly, Table 9 shows the results obtained for the multiple range test, which complements the discussion of the results.

Table 9 shows a general trend in which the composites with higher amounts of EPS in solution added obtained a lower mass variation (both in the dosages with and without fibres), which means that the amount of water absorbed by the samples was lower. The greatest decrease in mass variation is seen in the E0.7–450 dosage, which is 30% lower than the reference plaster. On this occasion, the analysis of Table 9 for the formation of homogeneous groups shows that there are statistically significant differences between the three proportions of EPS solution incorporated in the plaster composites developed. In the case of the incorporation of textile fibres in the composites, the slight increase in water absorption produced by the addition of these fibres in the plaster is again neutralised in the dosages that incorporate EPS solution in their composition. Although the fibres increase the variation in mass variation of water absorbed by 0.3–0.9% compared to the composites without fibres, this effect is not statistically significant. These results highlight the high impermeability of the developed composites in comparison to other studies where good results were obtained, where the plaster composites with the lowest water absorption varied in mass by 30–14% after this test [18,20,57]. Thus, as highlighted by Venkatesan *et al.*, increased impermeability of plaster composites would have a positive impact on increasing their durability and hindering bacterial growth [58].

3.4. Water vapour permeability

Table 10 presents the calculated values for water vapour transmission rate and water vapour permeance from which Fig. 8 has been derived, showing the results obtained for the variation in water vapour permeability determined over eight weeks of testing.

Generally speaking, the samples with dissolved EPS incorporation had a lower permeability to water vapour during the eight weeks in which the test was carried out. The lowest permeability was observed in E0.7–450, which contains the highest amount of dissolved EPS, being on average 17.44% less permeable than the plaster without additions. The E0.7–150 and E0.7–300 specimens showed similar results, with the E0.7–300 dosage registering a slightly higher vapour permeability than the reference plaster at weeks 6 and 7. As can be seen in Fig. 8, there is a strong increase in permeability up to week 4 in all the composites, this is due to the saturation period that the plaster undergoes during the first weeks, once the material is saturated the permeability drops drastically [59].

Table 9
Multiple Range Test for total water absorption.

Factor	Levels	LS Mean	LS Sigma	Homogeneus Group
Dossage	450	12.83	1.2971	X
	300	21.50		X
	150	63.67		X
	0	100.50		X
Fibers	NF	49–92	1.0068	X
	WF	49.33		X

Table 10
Water vapour transmission rate (WVT) and water vapour permeance (WVP) after eight weeks.

Sample	WVT (g/h·m^2)	PR (g/h·m^2·mmHg)
E0.7 (Ref.)	2,7600	0,3361
E0.7–150	2,7668	0,3369
E0.7–300	3,0487	0,3713
E0.7–450	2,7909	0,3399
E0.7-N	3,1758	0,3867
E0.7–150-N	2,6500	0,3227
E0.7–300-N	2,8906	0,3520
E0.7–450-N	2,2478	0,2737

The incorporation of textile fibres in the E0.7-N sample slightly increases the water vapour permeability of the plaster without additions. This behaviour is also observed in the E0.7–150-N composite, which obtained a higher permeability than its equivalent without textile fibres. However, with higher amounts of dissolved EPS (E0.7–300-N and E0.7–450-N), the permeability is reduced, even below the plasters containing only EPS in solution without ELT textile fibre. The low water vapour permeability of these compounds can be of interest in spaces with high humidity levels, where there is a significant risk of interstitial condensation that can lead to the deterioration of cladding and construction systems [60].

3.5. Karsten tube penetration test

Figs. 9 and 10 show the water penetration test results of the plaster composites with dissolved EPS and dissolved EPS and textile fibres respectively.

As can be seen in Fig. 9, all the plaster composites that incorporated the EPS solution managed to drastically reduce the amount of water penetrating through their surface compared to traditional plaster. The composites with the highest proportions of EPS in solution (E0.7–300 and E0.7–450) performed very similarly during the first half hour of testing, although the E0.7–300 plaster proved to be more impermeable to water, absorbing 93.8% less water than the reference plaster after one hour of exposure.

As can be seen in Fig. 10, the incorporation of textile fibres in the plaster (E0.7-N) reduced the permeability by 22.8% with respect to the reference plaster. The degree of waterproofing conferred by the synthetic textile fibres to the plaster is further enhanced by the combination of dissolved EPS, with increasingly lower permeabilities being obtained in this case as the amount of EPS increases. The lowest water absorption per minute is observed in the E0.7–450-N composite, being 97.8% lower than the plaster without additions (E0.7). These results agree with those

Table 8
Results of total water absorption of plaster composites.

Sample	E0.7	E0.7–150	E0.7–300	E0.7–450	E0.7-N	E0.7–150-N	E0.7–300-N	E0.7–450-N
Water absorption (%)	36.2	25.6	11.1	6.2	37.5	25.3	8.9	7.1

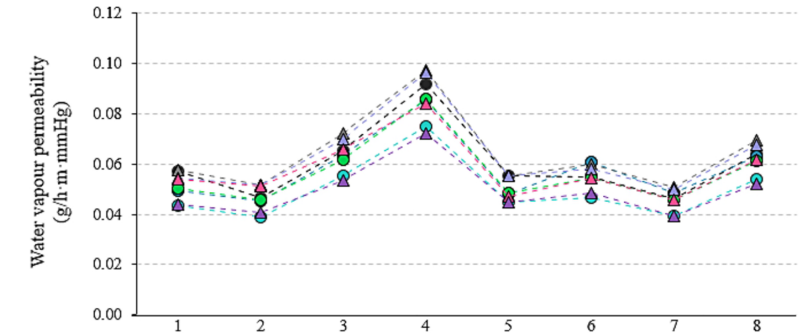

	1	2	3	4	5	6	7	8
E0.7	0.0570	0.0468	0.0651	0.0918	0.0553	0.0550	0.0460	0.0639
E0.7-450	0.0433	0.0391	0.0551	0.0747	0.0449	0.0465	0.0395	0.0539
E0.7-300	0.0492	0.0451	0.0636	0.0854	0.0481	0.0609	0.0487	0.0631
E0.7-150	0.0503	0.0455	0.0619	0.0860	0.0484	0.0545	0.0457	0.0612
E0.7-N	0.0576	0.0518	0.0719	0.0973	0.0555	0.0598	0.0507	0.0696
E0.7-150-N	0.0546	0.0516	0.0701	0.0964	0.0553	0.0579	0.0499	0.0678
E0.7-300-N	0.0540	0.0513	0.0658	0.0839	0.0473	0.0542	0.0457	0.0616
E0.7-450-N	0.0438	0.0407	0.0536	0.0721	0.0446	0.0483	0.0393	0.0520

Fig. 8. Water vapour permeability of composites for 8 weeks.

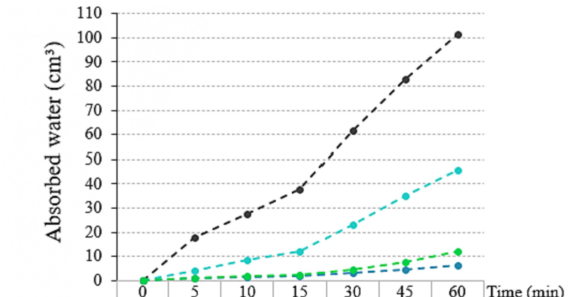

	0	5	10	15	30	45	60
E0.7	0	18	27.7	37.7	61.7	82.7	101.3
E0.7-150	0	4	8.5	12.1	23	35	45.9
E0.7-300	0	1	1.5	1.9	3.3	4.8	6.3
E0.7-450	0	1	1.9	2.6	4.5	7.7	12.1

Fig. 9. Surface water penetration test results for compounds E0.7, E0.7–150, E0.7–300 and E0.7–450.

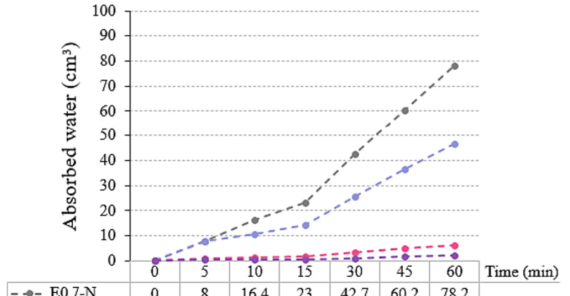

	0	5	10	15	30	45	60
E0.7-N	0	8	16.4	23	42.7	60.2	78.2
E0.7-150-N	0	8	10.7	14.4	25.4	36.5	46.7
E0.7-300-N	0	1	1.3	1.8	3.4	4.9	6.3
E0.7-450-N	0	0.4	0.4	0.5	1.1	1.7	2.2

Fig. 10. Surface water penetration test results of the compounds E0.7-N, E0.7–150-N, E0.7–300-N and E0.7–450-N.

obtained in Table 8 for the total water absorption test where the same trend could be observed.

3.6. Water-Stove cycles

In order to determine the deterioration produced by water on the plaster composites produced in this research, accelerated ageing tests were carried out. To this end, a series of samples subjected to water-stove cycles were used and another series of control samples were taken for each dosage developed. The same tests were carried out on both series: surface hardness, flexural strength and compressive strength, as well as recording the loss of mass experienced by the samples subjected to the durability cycles. The results obtained are shown in Table 11.

In addition, Table 12 shows the statistical analysis of the results obtained for the mechanical properties using the average of three series of specimens of each type (with and without cycles). An ANOVA of the results and a homogeneous group (HG) analysis have been performed with the total available data to support the discussion of these tests. To carry out this analysis, the mean differences obtained for the results between the three series of control specimens and the three series of specimens subjected to cycles were taken as the starting data.

As can be seen in Table 11, after the water and oven cycles, all the composites produced experienced a smaller variation in mass compared to the reference plaster. Nevertheless, those composites incorporating ELT textile fibers retained their mass more than their counterparts without fibers. On the other hand, it can be observed how the progressive partial replacement of the original plaster material by the dissolution of EPS residues increases the dimensional stability of the composites subjected to cycling. Thus, as can be seen in Table 11, the dosages with the addition of 450 g of dissolved EPS residue experienced the lowest percentage mass loss at the end of the accelerated ageing test.

Likewise, the surface hardness of the control composites decreases as the amount of added EPS residue solution increases, being even lower with the addition of ELT textile fibres. The most unfavourable case is observed for sample E0.7–450-N, with a reduction of 25.3%. After cycling, the surface hardness of the composites decreased to a greater extent as the amount of EPS increased, up to 18.46% in the case of the E0.7–450 dosage. Again, the incorporation of the textile fibres contributed to a reduction in the deterioration of the surface hardness of the samples with respect to their equivalents without fibres, although, as

Table 11
Weight, surface hardness, flexural and compressive strength results for control samples and samples subjected to cycles.

	Weight (g)			Surface hardness (Shore C units)			Flexural strength (MPa)			Compressive strength (MPa)		
Sample	Before test	Tested samples	Δ%	Control	Tested samples	Δ%	Control	Tested samples	Δ%	Control	Tested samples	Δ%
E0.7 (Ref.)	273.97	268.46	2.45	83	75	9.64	5.27	4.41	16.32	12.71	8.96	29.50
E0.7–150	250.67	245.70	1.98	78	70	10.26	5.11	4.38	14.29	9.39	6.52	30.56
E0.7–300	219.46	214.18	1.53	74	62	16.22	4.56	4.13	9.43	8.24	5.71	30.70
E0.7–450	191.22	185.50	1.42	65	53	18.46	3.87	3.53	8.79	6.41	4.21	34.32
E0.7-N	270.58	267.83	2.13	69	67	2.90	5.02	3.79	24.50	7.55	5.34	29.27
E0.7–150-N	249.09	246.49	1.85	66	63	4.55	4.67	4.15	11.13	8.4	5.56	33.81
E0.7–300-N	216.91	212.88	1.40	64	61	4.69	4.24	3.89	8.25	6.78	4.35	35.84
E0.7–450-N	193.50	189.72	1.28	62	57	8.06	3.95	3.69	6.58	6.21	3.75	39.61

Table 12
Statistical analysis for the difference of means between the results obtained for the samples subjected to water-stove cycles and the series of control samples.

Analysis of Variance (ANOVA)

Surface Hardness (Shore C unit)		Flexural Strength (MPa)		Compressive Strength (MPa)	
Dosage	Fibers	Dosage	Fibers	Dosage	Fibers
p-value: 0.1308	p-value: 0.2330	p-value: 0.0128	p-value: 0.0107	p-value: 0.0044	p-value: 0.0071

Multiple Range test for Water-Stove Cycles (Factor: Dosage)

Surface Hardness (Shore C unit)				Flexural Strength (MPa)				Compressive Strength (MPa)			
Level	Mean	Sigma	HG	Level	Mean	Sigma	HG	Level	Mean	Sigma	HG
450	2.67	0.6765	X	450	0.2500	0.1048	X	450	0.51	0.1032	X
300	4.17		XX	300	0.3050		X	300	0.68		X
0	4.67		XX	150	0.6283		X	0	0.69		X
150	4.83		X	0	0.7033		X	150	1.11		X

Multiple Range test for Water-Stove Cycles (Factor: Fibers)

Surface Hardness (Shore C unit)				Flexural Strength (MPa)				Compressive Strength (MPa)			
Level	Mean	Sigma	HG	Level	Mean	Sigma	HG	Level	Mean	Sigma	HG
NF	3.67	0.4783	X	NF	0.3233	0.7412	X	WF	0.59	0.0730	X
WF	4.50		X	WF	0.6200		X	NF	0.90		X

shown in Table 12, there were no statistically significant differences for either of the two factors included in the statistical analysis.

On the other hand, the addition of the EPS solution produced a decrement in the mechanical strength of the control samples in proportion to the amount of residue incorporated, being lower in the samples to which ELT textile fibers were added. However, after cycling, the composites showed an inverse behaviour in terms of strength loss. Contrary to other studies, where the incorporation of plastic residues contributed to a reduction in flexural strength of up to 40% after water-stove cycling [22], the plaster materials designed for this research that incorporated a higher amount of dissolved EPS residue and ELT textile fibers experienced the least loss of strength. The E0.7–450 and E0.7–450-N composites showed higher durability against cycling, whose reduction in flexural strength was 9.91% and 9.74% lower than the reference (E0.7) respectively.

Regarding the compressive strength test, it can be observed that the progressive substitution of the original plaster material by the dissolution of EPS residue decreases the compressive strength, which is in accordance with other studies where lightened plaster composites are developed and demonstrates the relationship between density reduction and compressive strength [61]. In the plaster composites subjected to water-stove cycles, a strong decrease in strength can be seen with respect to the control series of samples. This decrease in compressive strength is more pronounced in the composites with the addition of ELT textile fibers, this being a statistically significant factor as can be seen in Table 12. Thus, it can be stated that the addition of fibres improves only the flexural behaviour of the composites tested.

The good durability results of the lightened plasters with dissolved EPS and ELT textile fibres, with a reduced loss of mass and resistance to bending after being subjected to water and oven cycles, show the great potential of these new composites developed for the production of prefabricated ceiling panels and their application in spaces with high levels of humidity in buildings.

3.7. Scanning electron microscopy (SEM)

SEM images are helpful in supporting and complementing the results presented in this study. Fig. 11 shows the SEM images obtained for the compounds E0.7 (Reference), E0.7–450, E0.7-N and E0.7–450-N, these dosages are considered the most representative of all those elaborated as they present the greatest differences between them in terms of composition.

In Fig. 11 (a), the compact structure of needle-shaped dihydrate crystals characteristic of traditional plasters can be observed [62]. Fig. 11 (b), on the other hand, shows a much more porous plaster matrix, as confirmed by the mercury porosimetry results. Likewise, it can be observed how the EPS solution is able to enter inside the pores, resulting in two situations, either creating a thin film that coats the pores internally, or filling the pores [20]. This disposition of the EPS once solidified, obstructing some pores, would be blocking the access of water to the interior of the structure of the plaster material, making it more impermeable. On the other hand, this EPS solution film would be causing a decrease of interlocks between the calcium sulphate dihydrate crystals, which would be related to the progressive decrease of the mechanical strength of the plaster composites as the percentage of EPS solution addition increases in partial substitution of the original material [63].

Fig. 11 (c) shows one of the ELT textile fibres embedded in the plaster matrix. Some traces of adhered crystals can be observed on the fibre, which would indicate the good adhesion of this recycled material to the matrix. Finally, Fig. 11 (d) shows both the fibres contained in the sample, totally embedded in the plaster matrix, and pores partially covered by the solidified EPS inside. Likewise, the coating of the plaster crystals by the dissolved EPS would explain the high durability of the composites

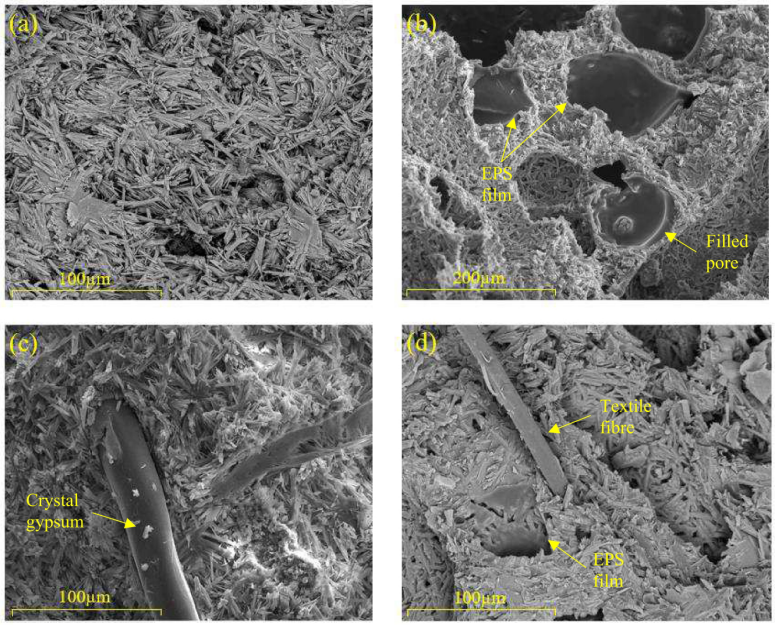

Fig. 11. Scanning electron microscopy (SEM): (a) Sample E0.7, magnifications x500; (b) Sample E0.7–450, magnifications x250; (c) Sample E0.7-N, magnifications x500; (d) Sample E0.7–450-N, magnifications x500.

developed, since the EPS would be enveloping and protecting these crystals from the deterioration caused by the water-stove cycles carried out.

In both samples E0.7–450 (Fig. 11 (b)) and E0.7–450-N (Fig. 11 (d)), the gypsum crystals show a less sharp morphology, which suggests that the incorporation of EPS dissolved in the plaster acts as a binder, coating the crystals and generating shorter and wider structures [19,64]. It can also be observed that in the samples where the EPS solution is incorporated (Fig. 11 (b) and (d)), the orientations of the plaster crystals are more limited, while in the traditional plaster (Fig. 11 (a)) the crystals form freely in all directions, which would have an effect on the slight decrease in the mechanical strength of the lightened composites.

3.8. Critical review and implications of the results obtained

Water is an aggressive agent capable of dissolving the gypsum crystals present in plaster and causing significant damage to the material [10]. This is why, traditionally, the use of plaster has been very limited in spaces with high levels of humidity [65]. In this research, a new lightweight plaster material highly resistant to water has been developed by incorporating a solution of recycled EPS and ELT textile fibres. The results obtained show how the addition of EPS in its liquid state and the incorporation of ELT textile fibres generate a very porous material with a low density, while at the same time greatly increasing the resistance of the plaster to the external action of water and achieving good physical and mechanical properties.

In this research work, it has been possible to verify how the progressive partial substitution of the original plaster material by EPS solution allows to increase the volume of pores in the composites produced, decreasing their apparent density and reflecting the suitability of these new materials for the production of lightweight prefabricated products. This is a point of great relevance, as in other investigations the incorporation of lightweight plastic waste had already been carried out in granular form, so this work opens up a new possibility for the recovery of EPS waste that allows improving the integration of the waste in the matrix of the original conglomerating material [45]. This combination between the EPS solution and the original plaster material has been observed in detail in the SEM analysis, which shows a homogeneous matrix and good cohesion between it and the NFU textile fibres.

On the other hand, it has been observed how the new materials developed in this research have shown an improved behaviour against the action of water as the main aggressive agent of gypsum composites. In this sense, the absorption of water by capillarity has been reduced, as well as the penetration of surface water and the permeability to water vapour, this effect being more significant in the composites with a greater amount of raw material incorporated. In the same way, all the composites developed in this research have performed well in accelerated ageing cycles, always exceeding the minimum values for mechanical resistance established by current regulations. Moreover, after these durability tests, the new plaster materials designed have shown excellent dimensional stability, contrary to what has occurred in other research using additions of solid waste in the form of aggregates [66].

4. Conclusions

The waterproof behaviour of the plaster composites developed in this research greatly expands the field of application that plaster materials have traditionally had in building construction. The plaster composites incorporating dissolved EPS and ELT textile fibres are presented as a technically viable alternative to produce prefabricated panels and slabs for use in wet rooms, while promoting a responsible use of resources by reducing the consumption of natural raw materials and the reincorporation of waste in the production process of this new sustainable building material. In this way, after the experimental program carried out, the following main conclusions can be drawn:

- The porosity of the plasters increases as the amount of dissolved EPS waste increases, with the E0.7–450 sample being up to 10.82% more porous compared to the reference sample. However, the incorporation of ELT textile fibres slightly reduced this porosity, generating pores of smaller dimensions than those observed in the plasters

containing only EPS in solution. However, all the composites produced obtained a higher porosity than the reference plaster without additions (E0.7).

- Both capillary water absorption and total water absorption decrease as the amount of recycled EPS dissolved in the samples increases. A maximum reduction of around 30% was obtained in both tests for the samples with the highest content of dissolved EPS added. It has been observed how the incorporation of ELT textile fibres slightly increases water absorption, however, when combining the fibres with the EPS solution, absorption decreases again as the proportion of EPS increases, reaching values close to those obtained for the composites without fibres. This behaviour highlights the suitability of EPS waste in solution to control water absorption in humid environments in hardened plaster composites. This behaviour highlights the suitability of EPS waste in solution to control water absorption in humid environments in hardened plaster composites.
- The composites with a higher proportion of dissolved EPS (E0.7–450 and E0.7–450-N) had the lowest water vapour permeability among all the plasters produced in this study, between 15.5% and 18.6% lower than the plaster without additions (E0.7).
- All the composites developed showed a surface water absorption much lower than that of the plaster without additions. The lowest water penetration was obtained in the E0.7–450-N dosage, being 97.8% lower than traditional plaster (E0.7).
- The composites developed in this research showed increased stability after accelerated ageing cycles compared to the reference plaster. The addition of dissolved recycled EPS and ELT textile fibres approximately halved the mass loss as the amount of recycled material added increased. Likewise, the loss of surface hardness and flexural strength was also lower in the composites incorporating both additions. In any case, all the composites tested showed flexural and compressive strengths above 1 MPa and 2 MPa respectively, in compliance with the recommendations of current European standards.
- SEM images show how the dissolved EPS is able to fully integrate into the plaster material, creating a matrix with a high cohesion between its components. Likewise, the ELT textile fibres show good adhesion with the matrix of the developed plaster composites.

The main limitations of this research are the following: (1) lack of substitution percentages of intermediate EPS solution that would have enriched the statistical discussion; (2) due to the sample size, regression models have not been carried out to describe in detail the water behaviour of these new materials; (3) with the equipment available in the laboratory, it has not been possible to carry out full-scale tests on plates and panels for modular construction.

Finally, as future lines of work to give continuity to the study carried out with the new plaster composites presented, the following are highlighted: (1) carrying out an instrumental analysis of these new composites developed and thus complementing the chemical characterisation; (2) carrying out tests to determine the growth of fungi in humid environments on the surface of these materials; (3) using infrared thermography in capillary absorption tests to determine more precisely the distribution of water inside the plaster matrix, and, (4) carrying out durability tests in repeated wet chamber cycles to complement the physical–mechanical characterisation of these materials.

CRediT authorship contribution statement

Alicia Zaragoza-Benzal: Conceptualization, Data curation, Formal analysis, Investigation, Methodology, Resources, Software, Validation, Visualization, Writing – original draft, Writing – review & editing. **Daniel Ferrández:** Conceptualization, Data curation, Funding acquisition, Investigation, Project administration, Resources, Supervision, Validation, Writing – review & editing. **Evangelina Atanes-Sánchez:** Data curation, Formal analysis, Investigation, Methodology, Resources, Software, Supervision, Writing – review & editing. **Pablo Saíz:** Data curation, Investigation, Software, Supervision, Writing – review & editing.

Declaration of Competing Interest

The authors declare that they have no known competing financial interests or personal relationships that could have appeared to influence the work reported in this paper.

Data availability

The authors do not have permission to share data.

Acknowledgements

The authors would like to express their gratitude to the firm SIGNUS ECOVALOR S.L. for its close collaboration, great interest, and considerable support for this research work, as well as for raising awareness and searching for new solutions for the proper management of end-of-life tyres.

References

[1] B. Qi, M. Razkenari, A. Costin, C. Kibert, M. Fu, A systematic review of emerging technologies in industrialized construction, J. Build. Eng. 39 (. 2021), 102265, https://doi.org/10.1016/J.JOBE.2021.102265.
[2] A.O. Sojobi, A.H. Alavi, Evaluation of the performance of eco-friendly lightweight interlocking concrete paving units incorporating sawdust wastes and laterite, Cogent Eng 3 (1) (2016) 1255168.
[3] European Commission, "A more resilient, green and digital construction ecosystem." https://single-market-economy.ec.europa.eu/sectors/construction/construction-transition-pathway_en (accessed Mar. 27, 2023).
[4] T. Alomayri, A. Raza, F. Shaikh, Effect of nano SiO2 on mechanical properties of micro-steel fibers reinforced geopolymer composites, Ceram. Int. 47 (23) (2021) 33444–33453, https://doi.org/10.1016/j.ceramint.2021.08.251.
[5] A.B. Elhag, et al., A critical review on mechanical, durability, and microstructural properties of industrial by-product-based geopolymer composites, Rev. Adv. Mater. Sci. 62 (1) (2023), https://doi.org/10.1515/rams-2022-0306.
[6] United Nations General Assembly, "Transforming our world: the 2030 Agenda for Sustainable Development Agenda for Sustainable Development." 2015. Accessed: Oct. 05, 2022. [Online]. Available: https://sdgs.un.org/.
[7] J.I. Escalante-Garcia, O.A. Martínez-Aguilar, L.Y. Gomez-Zamorano, Calcium sulphate anhydrite based composite binders; effect of Portland cement and four pozzolans on the hydration and strength, Cem. Concr. Compos. 82 (2017) 227–233, https://doi.org/10.1016/J.CEMCONCOMP.2017.05.012.
[8] B. Srinivasaraonaik, L.P. Singh, S. Sinha, I. Tyagi, A. Rawat, Studies on the mechanical properties and thermal behavior of microencapsulated eutectic mixture in gypsum composite board for thermal regulation in the buildings, J. Build. Eng. 31 (2020), 101400, https://doi.org/10.1016/J.JOBE.2020.101400.
[9] D.D.C.V. Sheng, N.S. Ramegowda, V. Guna, N. Reddy, Groundnut shell and coir reinforced hybrid bio composites as alternative to gypsum ceiling tiles, J. Build. Eng. 57 (2022), 104892, https://doi.org/10.1016/J.JOBE.2022.104892.
[10] C. Caselle, P. Baud, A.R.L. Kushnir, T. Reuschlé, S.M.R. Bonetto, Influence of water on deformation and failure of gypsum rock, J. Struct. Geol. 163 (Oct. 2022), 104722, https://doi.org/10.1016/j.jsg.2022.104722.
[11] C. Chen, F. Ma, T. He, Z. Kang, Y. Wang, C. Shi, Improved water and efflorescence resistance of flue gas desulfurization gypsum-based composites by generating hydrophobic coatings, J. Clean. Prod. 371 (2022) 133711.
[12] Y. Kang, S.J. Chang, S. Kim, Hygrothermal behavior evaluation of walls improving heat and moisture performance on gypsum boards by adding porous materials, Energ. Buildings 165 (2018) 431–439, https://doi.org/10.1016/J.ENBUILD.2017.12.052.
[13] A. Çolak, Characteristics of acrylic latex-modified and partially epoxy-impregnated gypsum, Cem. Concr. Res. 31 (11) (2001) 1539–1547, https://doi.org/10.1016/S0008-8846(01)00575-0.
[14] N. Sakthieswaran, M. Sophia, Effect of superplasticizers on the properties of latex modified gypsum plaster, Constr. Build. Mater. 179 (2018) 675–691, https://doi.org/10.1016/J.CONBUILDMAT.2018.05.150.
[15] Z. Li, X. Wang, Y. Hou, Z. Wu, Optimization of mechanical properties and water absorption behavior of building gypsum by ternary matrix mixture, Constr. Build. Mater. 350 (2022), 128910, https://doi.org/10.1016/J.CONBUILDMAT.2022.128910.
[16] M. Doleželová, J. Krejsová, L. Scheinherrová, M. Keppert, A. Vimmrová, Investigation of environmentally friendly gypsum based composites with improved water resistance, J. Clean. Prod. 370 (2022) 133278.
[17] Q. Wang, Y. Cui, J. Xue, Study on the improvement of the waterproof and mechanical properties of hemihydrate phosphogypsum-based foam insulation

materials, Constr. Build. Mater. 230 (2020), 117014, https://doi.org/10.1016/J.CONBUILDMAT.2019.117014.
[18] A. Pundir, M. Garg, R. Singh, Evaluation of properties of gypsum plaster-superplasticizer blends of improved performance, J. Build. Eng. 4 (2015) 223–230, https://doi.org/10.1016/J.JOBE.2015.09.012.
[19] D. López Pedrajas, M. Carmona Franco, I. Garrido Sáenz, F.J. Ramos Mellado, J. F. Rodríguez Romero, A.M. Borreguero Simón, Polystyrene nanoparticles slurry as an additive for developing insulating and waterproof gypsum composites, Appl. Therm. Eng. 217 (2022), https://doi.org/10.1016/J.APPLTHERMALENG.2022.119271.
[20] Q. Wu, H. Ma, Q. Chen, B. Gu, S. Li, H. Zhu, Effect of silane modified styrene-acrylic emulsion on the waterproof properties of flue gas desulfurization gypsum, Constr. Build. Mater. 197 (2019) 506–512, https://doi.org/10.1016/J.CONBUILDMAT.2018.11.185.
[21] P.O. Awoyera, O.B. Olalusi, D.P. Babagbale, O.E. Babalola, A review of lightweight composite development using paper waste and pulverized ceramics - towards a sustainable and eco-friendly construction, Int. J. Eng. Res. Afr. 56 (Oct. 2021) 77–94, https://doi.org/10.4028/www.scientific.net/JERA.56.77.
[22] A. Vidales-Barriguete, E. Atanes-Sánchez, M. del Río-Merino, C. Piña-Ramírez, Analysis of the improved water-resistant properties of plaster compounds with the addition of plastic waste, Constr. Build. Mater. 230 (2020), https://doi.org/10.1016/J.CONBUILDMAT.2019.116956, 116956.
[23] M.I. Romero-Gómez, R.V. Silva, I. Flores-Colen, J. de Brito, Influence of polypropylene residues on the physico-mechanical and water-resistance properties of gypsum plasters, J. Clean. Prod. 371 (2022), 133674, https://doi.org/10.1016/J.JCLEPRO.2022.133674.
[24] M. Sophia, N. Sakthieswaran, Waste shell powders as valuable bio- filler in gypsum plaster – Efficient waste management technique by effective utilization, J. Clean. Prod. 220 (2019) 74–86, https://doi.org/10.1016/J.JCLEPRO.2019.02.119.
[25] E.M. Tuuri, S.C. Leterme, How plastic debris and associated chemicals impact the marine food web: A review, Environ. Pollut. 321 (2023) 121156.
[26] L. Prasittisopin, P. Termkhajornkit, Y.H. Kim, Review of concrete with expanded polystyrene (EPS): Performance and environmental aspects, J. Clean. Prod. 366 (2022), 132919, https://doi.org/10.1016/j.jclepro.2022.132919.
[27] J. Schleier, M. Simons, K. Greiff, G. Walther, End-of-life treatment of EPS-based building insulation material – An estimation of future waste and review of treatment options, Resour. Conserv. Recycl. 187 (2022), 106603, https://doi.org/10.1016/J.RESCONREC.2022.106603.
[28] A. Milling, A. Mwasha, H. Martin, Exploring the full replacement of cement with expanded polystyrene (EPS) waste in mortars used for masonry construction, Constr. Build. Mater. 253 (2020) 119158.
[29] T. Fehn, F. Kugler, B. Tübke, R. Schweppe, P. Mebert, W. Krcmar, U. Teipel, Charakterisierung und Störstoffanalyse von rückgewonnenen Stoffströmen aus Wärmedämmverbundsystemen, Chem. Ing. Tech. 93 (5) (2021) 771–780.
[30] S. Bouzit, F. Merli, M. Sonebi, C. Buratti, M. Taha, Gypsum-plasters mixed with polystyrene balls for building insulation: Experimental characterization and energy performance, Constr. Build. Mater. 283 (2021) 122625.
[31] K.A. de Oliveira, C.A.B. Oliveira, J.C. Molina, Lightweight recycled gypsum with residues of expanded polystyrene and cellulose fiber to improve thermal properties of gypsum, Mater. Constr. 71 (341) (2021) e242–e, https://doi.org/10.3989/MC.2021.07520.
[32] Z. Xiao, A. Pramanik, A.K. Basak, C. Prakash, S. Shankar, Material recovery and recycling of waste tyres-A review, Cleaner Materials 5 (2022), 100115, https://doi.org/10.1016/j.clema.2022.100115.
[33] D. Landi, S. Gigli, M. Germani, M. Marconi, Investigating the feasibility of a reuse scenario for textile fibres recovered from end-of-life tyres, Waste Manag. 75 (2018) 187–204, https://doi.org/10.1016/J.WASMAN.2018.02.018.
[34] L.G. Picado-Santos, S.D. Capitão, J.M.C. Neves, Crumb rubber asphalt mixtures: A literature review, Constr. Build. Mater. 247 (2020), 118577, https://doi.org/10.1016/J.CONBUILDMAT.2020.118577.
[35] Q.B. Thai, K. Le-Cao, P.T.T. Nguyen, P.K. Le, N. Phan-Thien, H.M. Duong, Fabrication and optimization of multifunctional nanoporous aerogels using recycled textile fibers from car tire wastes for oil-spill cleaning, heat-insulating and sound absorbing applications, Colloids Surf A Physicochem Eng Asp 628 (2021), 127363, https://doi.org/10.1016/J.COLSURFA.2021.127363.
[36] D. Ferrández, A. Zaragoza, and C. Morón, "Material de construcción aislante aligerado, panel o placa prefabricado, proceso de elaboración de dicho material de construcción y de dicho panel o placa prefabricado," P202230251, 2022.
[37] UNE-EN 13279-1:2009, "Yesos de construcción y conglomerantes a base de yeso para la construcción. Parte 1: Definiciones y especificaciones." 2009.
[38] Saint-Gobain Placo, "Iberyola granel. Yesos y Plastes." https://www.placo.es/documents/ficha-tecnica/ft-placo-iberyola-granel-es.pdf (accessed May 19, 2023).
[39] Asociación Nacional de Poliestireno Expandido (ANAPE), "Construcción sostenible." www.anape.es (accessed Jul. 12, 2022).
[40] A.M. Papadopoulos, State of the art in thermal insulation materials and aims for future developments, Energ. Build. 37 (1) (2005) 77–86, https://doi.org/10.1016/J.ENBUILD.2004.05.006.
[41] Nazza, "Ficha Técnica: Disolvente multiusos." 2020. Accessed: Dec. 27, 2021. [Online]. Available: https://www.nazza.es/img/cms/documentos%20PDF/Fichas%20T%C3%A9cnicas/FT%20-%20Disolvente%20multiusos%20Nazza.pdf.
[42] V.L. Shulman, Chapter 21 - tyre recycling, in: Waste. A Handbook for Management, Academic Press, 2011, pp. 297–320, doi: 10.1016/B978-0-12-381475-3.10021-X.
[43] D. Landi, S. Vitali, M. Germani, Environmental analysis of different end of life scenarios of tires textile fibers, Procedia CIRP 48 (Jan. 2016) 508–513, https://doi.org/10.1016/J.PROCIR.2016.03.141.
[44] M. Álvarez, D. Ferrández, C. Morón, E. Atanes-Sánchez,, Characterization of a new lightened gypsum-based material reinforced with fibers, Materials 14 (2021) 1203, https://doi.org/10.3390/MA14051203.
[45] M. del Rio Merino, P. Villoria Sáez, I. Longobardi, J. Santa Cruz Astorqui, C. Porras-Amores, Redesigning lightweight gypsum with mixes of polystyrene waste from construction and demolition waste, J. Clean. Prod. 220 (2019) 144–151.
[46] A. Vidales Barriguete, M. del Río Merino, E. Atanes Sánchez, C. Piña Ramírez, C. Viñas Arrebola, Analysis of the feasibility of the use of CDW as a low-environmental-impact aggregate in conglomerates, Constr. Build. Mater. 178 (2018) 83–91.
[47] UNE-EN 13279-2:2014, "Yesos de construcción y conglomerantes a base de yeso para la construcción. Parte 2: Métodos de ensayo." 2014.
[48] European Commission, "The European Green Pact." 2019. [Online]. Available: https://sustainabledevelopment.un.org/post2015/transformingourworld.
[49] S.G. Morales, Metodología de diagnóstico de humedades de capilaridad ascendente y condensación higroscópica en edificios históricos, Universidad Politécnica de Madrid, Madrid, Spain, 1995.
[50] RILEM RC 25-PEM, "Recommended test to measure the deterioration of stone and to assess the effectiveness of treatment methods.," *Materials and Structures*, vol. 13, no. 75. pp. 175–253, 1980.
[51] UNE-EN 520:2005+A1, "Placas de yeso laminado. Definiciones, especificaciones y métodos de ensayo.," 2010.
[52] UNE-EN ISO 12572, "Prestaciones higrotérmicas de los productos y materiales para edificación. Determinación de las propiedades de transmisión de vapor de agua. Método del vaso," 2018.
[53] RILEM, "Water absorption under low pressure. Pipe method. Test n° II. 4, Tentative Recommendations.," Paris, 1980.
[54] M. del Río Merino, "Elaboración y aplicaciones constructivas de paneles prefabricados de escayola aligerada y reforzada con fibras de vidrio E y otros aditivos," Universidad Politécnica de Madrid, Madrid, Spain, 1999. doi: 10.20868/UPM.thesis.612.
[55] L.B. McCusker, F. Liebau, G. Engelhardt, Nomenclature of structural and compositional characteristics of ordered microporous and mesoporous materials with inorganic hosts (IUPAC Recommendations 2001), Pure Appl. Chem. 73 (2) (2001) 381–394.
[56] O. López-Zaldívar, R. Lozano-Díez, S. Herrero del Cura, P. Mayor-Lobo, F. Hernández-Olivares, Effects of water absorption on the microstructure of plaster with end-of-life tire rubber mortars, Constr. Build. Mater. 150 (2017) 558–567, https://doi.org/10.1016/J.CONBUILDMAT.2017.06.014.
[57] Z. Li, K. Xu, J. Peng, J. Wang, J. Zhang, Q. Li, Study on mechanical strength and water resistance of organosilicon waterproofing agent blended recycled gypsum plaster, Case Stud. Constr. Mater. 14 (2021) e00546.
[58] B. Venkatesan, V. Kannan, M. Sophia, Application potentials of conch shell powder as a bacterial carrier for enhancing the Micro-Mechanical performance of biogenic gypsum plaster, Constr. Build. Mater. 399 (2023), 132561, https://doi.org/10.1016/j.conbuildmat.2023.132561.
[59] M. Álvarez, D. Ferrández, P. Guijarro-Miragaya, C. Morón, Characterization and under Water Action Behaviour of a New Plaster-Based Lightened Composites for Precast, Materials 16 (2) (2023) 872, https://doi.org/10.3390/MA16020872.
[60] M.Y. Durgun, Effect of wetting-drying cycles on gypsum plasters containing ground basaltic pumice and polypropylene fibers, J. Build. Eng. 32 (2020) 101801.
[61] M. del Río-Merino, A. Vidales-Barriguete, C. Piña-Ramírez, V. Vitiello, J. Santa Cruz-Astorqui, R. Castelluccio, A review of the research about gypsum mortars with waste aggregates, J. Build. Eng. 45 (2022) 103338.
[62] R.M. Gonçalves, A. Martinho, J.P. Oliveira, Evaluating the potential use of recycled glass fibers for the development of gypsum-based composites, Constr. Build. Mater. 321 (Feb. 2022), 126320, https://doi.org/10.1016/J.CONBUILDMAT.2022.126320.
[63] A. Zaragoza-Benzal, D. Ferrández, E. Atanes-Sánchez, P. Saíz, Dissolved recycled expanded polystyrene as partial replacement in plaster composites, J. Build. Eng. 65 (2023), 105697, https://doi.org/10.1016/j.jobe.2022.105697.
[64] Y. Zhang, J. Yang, X. Cao, Effects of several retarders on setting time and strength of building gypsum, Constr. Build. Mater. 240 (2020) 117927.
[65] M. Doleželová, L. Scheinherrová, J. Krejsová, M. Keppert, R. Černý, A. Vimmrová, Investigation of gypsum composites with different lightweight fillers, Constr. Build. Mater. 297 (2021), 123791, https://doi.org/10.1016/J.CONBUILDMAT.2021.123791.
[66] A. Vidales-Barriguete, E. Atanes-Sánchez, M. del Río-Merino, C. Piña-Ramírez, Analysis of the improved water-resistant properties of plaster compounds with the addition of plastic waste, Constr. Build. Mater. 230 (2020), 116956, https://doi.org/10.1016/J.CONBUILDMAT.2019.116956.

3.5. Fire-resistant performance of new sustainable waste-lightened composites with glass and basalt fibres reinforcement

Contents lists available at ScienceDirect

Construction and Building Materials

journal homepage: www.elsevier.com/locate/conbuildmat

Fire-resistant performance of new sustainable waste-lightened composites with glass and basalt fibres reinforcement

Alicia Zaragoza-Benzal [a,*], Daniel Ferrández [a], M. Isabel Prieto [a], Evangelina Atanes-Sánchez [b]

[a] Universidad Politécnica de Madrid, Departamento de Tecnología de la Edificación, 28040 Madrid, Spain
[b] Universidad Politécnica de Madrid, Departamento de Ingeniería Mecánica, Química y Diseño Industrial, 28012 Madrid, Spain

ARTICLE INFO

Keywords:
Lightweight plaster composites
Fire behaviour
Expanded polystyrene (EPS) waste
Raw material saving
Fibre reinforcement

ABSTRACT

In recent years, numerous studies have been conducted on the incorporation of plastic wastes into gypsum or plaster compounds with the aim of achieving more sustainable and environmentally friendly materials. Despite the vulnerability of plastic materials to high temperatures, it is not common to analyze the behavior of these new compounds in case of a fire. In this study, different lightweight plaster compounds have been developed, partially replacing the original raw materials with plastic waste in dissolution up to 23.5% and reinforced with glass and basalt fibers. After exposing the compounds to real direct fire, mechanical characterization (flexural strength, compressive strength, surface hardness tests) and physicochemical characterization (XRD, TGA) have been carried out, including the calculation of CO and CO_2 emissions associated with the combustion of the compounds, as well as imaging by scanning electron microscopy. The results show that the reduction in the density (between 15%−24%) of the new compounds favored lower temperatures during exposure to flames, preventing material cracking. Likewise, the new composites experienced a loss in flexural strength between 44%− 51%, and a drop in compressive strength between 2%− 63%, being these losses in strength lower than those experienced by the reference composites. The addition of glass fibers demonstrated to confer better flexural behaviour to the compounds with added waste, while the basalt fibers were more efficient in compression. Furthermore, the estimated toxic emissions produced during the combustion of the designed compounds did not exceed the immediately dangerous to life or health (IDLH) values established by the Material Safety Data Sheet (MSDS), remaining below 2000 ppm/h for CO and 40,000 ppm for CO_2. This study contributes to a better understanding of the behavior of plaster compounds with incorporation of plastic waste in case of fire, highlighting the developed materials as a viable alternative for the production of more environmentally friendly prefabricated products.

1. Introduction

The exponential growth in the consumption of plastic materials, coupled with the inefficient management of generated waste, has caused a worldwide alarm, becoming one of the most harmful activities for the environment and resulting in devastating consequences for ecosystems. The problem posed by these wastes, which potentially end up contaminating many natural areas in the form of micro and nano plastics, is compounded by the significant amount of greenhouse gas emissions produced during their manufacturing [1]. For this reason, it is not surprising that various sectors such as academia, legislation and institutions are moving towards a circular economy model with the aim of reversing this situation.

Recently, the reuse of plastic waste as a secondary raw material in the production of new sustainable construction materials is arousing great interest both in the research community and in the construction industry [2,3]. Specifically, in 2021, 18.1% (2364 kt) of recycled plastic was used in manufacturing new products in the EU construction sector, a figure that has been increasing year by year [4]. Polymers like expanded polystyrene (EPS) deserve special attention as its production is increasing exponentially in recent years worldwide (18.7 Mt in 2021 [4]), partly due to its use in renovation projects through External Thermal Insulation Composite System (ETICS). This material's high thermal resistance, great lightness, durability and low price make it an ideal insulator for energy-efficient building rehabilitation. However, the management of these waste in landfills represents a challenge due to its

* Corresponding author.
E-mail address: alicia.zaragoza@upm.es (A. Zaragoza-Benzal).

https://doi.org/10.1016/j.conbuildmat.2023.134620
Received 6 October 2023; Received in revised form 26 November 2023; Accepted 13 December 2023

large occupancy volumes, slow degradation process, strong visual impact and generation of microplastics [5–7].

In the quest to establish process innovations that advance towards sustainable construction and introduce close loop models during the construction phase, numerous research studies have proposed the recovery of EPS waste as a lightweight addition to reduce the specific weight and thermal conductivity of cement, gypsum or plaster-based composites. The vast majority of these studies explore the feasibility of incorporating recycled EPS aggregates as lightweight filler in binder materials, which generally leads to a large decrease in mechanical strength, segregation of the waste during the mixing process, as well as a weak bond between the EPS and the base material matrix [8–11]. As an alternative to these approaches found in the literature, this study introduces, in an original way, the EPS residue previously dissolved during the mixing process of plaster composites. This innovative method of waste reincorporation generates more cohesive and homogeneous composites, with high porosity and reduced thermal conductivity, while still achieving good mechanical performance and high durability [12]. However, EPS as a thermoplastic material is particularly vulnerable to high temperatures, making it essential to thoroughly understand the behaviour of composites designed using this novel manufacturing process in the event of a possible fire due to the material and personal damage that could be caused. The specific case of composites made of gypsum and plaster is particularly relevant since, in addition to being one of the main cladding materials in buildings, their high heat absorption capacity makes them a very interesting option as passive fire protection in different types of structures [13,14].

In the literature, no research has been found assessing the behaviour of gypsum or plaster composites with the incorporation of EPS waste at high temperatures, so, as a reference, the effects of high temperatures on gypsum materials with other plastics added have been consulted. Romero-Gomez *et al.* [15] observed how the melting point of polypropylene (PP) and nylon (PA6) waste influenced the residual strength of gypsum composites when subjected to temperatures of up to 300 °C. The best results were obtained with additions of 2.5 wt% PA6, which created a bridging effect after re-solidifying within the deteriorated matrix of the composites. Castellón *et al.* [16] evaluated the effects of incorporating tire rubber waste into gypsum composites after being exposed to temperatures of up to 830 °C. The authors observed that the rapid temperature increase generated by the decomposition of the waste contributed to the almost complete transformation of the dihydrate present in the composites into anhydrite, resulting in reductions of 55–85% in flexural strength and 54–86% in compressive strength. For their part, Vidales-Barriguete *et al.* [17] observed how the addition of plastic waste from cables caused significant deterioration in plaster composites after subjecting the materials to a real-fire test. However, in their research, it was noted that the plaster coating around the waste provided a physical protection that contributed to a slower degradation of the plastic waste.

Several investigations have been conducted on the incorporation of reinforcement fibres such as glass fibre (GF) or basalt fibre (BF) with the aim of enhancing the strength of these composites when subjected to fire conditions [18,19]. These inorganic fibres, in addition to improving the mechanical properties of the composites, are stable at very high temperatures elevadas [20,21]. Li *et al.* [22] incorporated glass and basalt fibres of different lengths in gypsum-based composites. Their best results were achieved with 1%wt addition of 10 mm length fibres, resulting in increases in flexural strength of about 70%. However, a progressive increase in volume and length of the fibres led to a proportional decrease in strength as well as in setting time. Du *et al.* [20] incorporated glass fibre (0.5–2 wt%) to enhance the integrity of gypsum composites after being exposed to 800 °C. The authors observed that the addition of 1 wt % glass fibre reduced the loss of mechanical strength by about 20% after reaching 400ºC. However, an increase in cracking was observed in the samples once the fibres reached their melting point. Likewise, Li *et al.* [21] added 0.5–1.0 wt% basalt fibres to improve the strength of gypsum composites with diatomite. The reinforced composites exhibited higher mechanical strengths than the reference up to 600 °C. The fibres were found to confer greater dimensional stability to the material, maintaining their integrity and significantly reducing the number of cracks in the specimens after reaching 300 °C.

Typically, the behaviour of composites tested at high temperatures is carried out in stoves or muffles with tightly controlled parameters, which do not represent the complex reality inherent to a fire. The stages of growth, development and end of a fire depend on the location and distribution of the ignition point, the quantity and type of combustible material, and the ventilation within the space. This diversity of factors undercores the importance of conducting tests that closely resemble a real fire to gain a holistic understanding of how materials behave in such incidents [23].

In some cases, the study of a construction material's behaviour under the action of fire by evaluating its residual mechanical capacity and mass loss is not sufficient for a complete characterisation. Knowing also the emission of harmful gases that are generated becomes a requirement since poisoning by inhalation of toxic gases represents the main cause of death in fires [24,25]. Considering the great impact that materials incorporating plastic waste can have in the form of harmful gas emissions during a fire, very little research has focused on this issue. In this regard, Romero-Gómez *et al.* [15] quantified various hazardous gases related to the combustion of plastic waste-containing gypsum composites using a series of sensors placed inside a muffle. Their results showed that incorporating 7.5 wt% PP waste released 7000 ppm CO_2, although this amount is below the values considered dangerous to health. In this case, it was not possible to record the emitted CO as complete combustion of the material occurred when a controlled temperature was applied. On the other hand, Vidales-Barriguete *et al.* [17] carried out a theoretical estimation of the emissions linked to the combustion of plaster composites incorporating plastic waste from cables at 50–60-70%. Based on data obtained from thermogravimetric analysis, it was estimated that in the case of incomplete combustion (releasing only CO), the harmful concentration for health was exceeded in all cases, while in the case of complete combustion (releasing only CO_2), the maximum concentration was around 16000 ppm, not reaching the hazardous values.

However, there are no studies in the literature that evaluate the release of harmful gases (CO and CO_2) that could cause health issues in humans during the combustion of gypsum or plaster composites incorporating EPS waste. To provide a reference framework, the study by Wi *et al.* [26] can be highlighted, where the fire behaviour of different polymeric thermal insulators was analysed. By evaluating the total heat release (THR) and heat release rate (HRR), the authors observed that all the insulators tested exceeded the immediately dangerous to life or health (IDLH) value for CO established by the Material Safety Data Sheet (MSDS) [27]. The highest levels of this gas were recorded during the combustion of Polyisocyanurate and Polyurethane foam, reaching approximately 20,000 ppm and 16,000 ppm respectively. In contrast, the highest CO_2 concentration was observed during the combustion of XPS and EPS, with 4693 ppm and 3540 ppm respectively, not exceeding the maximum value of 40,000 ppm of the IDLH.

In this context, following the literature review conducted, no studies have been found that analyse the behaviour of plaster composite materials with additions of recycled EPS under the action of a real fire. In this sense, the first objective was to develop new plaster materials incorporating EPS waste in dissolution to improve their integration in the matrix of the composites produced. Subsequently, the analysis of the fire behaviour by means of a direct real-fire test on the plaster materials produced, with and without synthetic fibre reinforcement (glass and basalt), has been proposed, with the intention of evaluating the effects of these commercial fibres on the new material. Once this test had been carried out, the aim was to analyse the mechanical resistance of the composites subjected to the action of fire, compared to the same plaster composites without being subjected to this destructive test, taking them

as a reference. Finally, to complete the study, a physicochemical analysis of the composites produced was carried out, estimating the CO and CO_2 emissions that would be released in fire conditions.

2. Materials and methods

2.1. Materials

The following raw materials were used to prepare the matrix of the composites proposed in the experimental campaign:

- E-35 plaster, designated as high purity and fineness type A gypsum according to UNE-EN 13279-1 standard [28], produced by Saint-Gobain Placo Ibérica (Madrid, Spain). It is classified A1 according to the European Reaction to Fire classification system, i.e. it is non-combustible and does not contribute to fire spread [29].
- Drinking and impurity-free water from the Canal de Isabel II, Madrid (Spain). This water has been used in numerous studies where its suitability in the elaboration of plaster composites has been proven [30,31].
- Expanded polystyrene (EPS) waste from energy-efficient facade rehabilitation in Madrid, Spain. This type of material is characterised by its low thermal conductivity (0.031 W/mK) and low density (28-30 kg/m^3) [32].
- Multipurpose solvent supplied by the company Nazza (Madrid, Spain), composed of toluene, xylene, n-butyl acetate, ethyl acetate, ethylbenzene, acetone, propan-2-one and propanone. The main properties of this material, provided by the manufacturer, are vapour pressure 85.5 mmHg at 20 °C and density at 20 °C (ASTM D 1298/4052) 812 ± 20 kg/m^3 [33].

On the other hand, the following reinforcement fibres have been used to improve the mechanical properties of these composite materials, following the criteria of similar density and good resistance to high temperatures. A fibre length of 12 mm has been selected, as this is a value commonly used in plaster composites and has given good results in previous work [34], [35]. The main characteristics of which are shown in Table 1:

- Glass fibre manufactured by Fiber Eagle S.A. (Madrid, Spain). This inorganic fibre is resistant to high temperatures, as well as to acids, and is characterised by low thermal and electrical conductivity [36].
- Basalt fibre supplied by Mapei S.A. (Barcelona, Spain). This type of fibre is inorganic, non-combustible and exhibit a high chemical stability. In addition, its manufacturing requires less energy compared to other reinforcing fibres and is easier to process [37].

2.2. Test sample preparation

In the process of preparing the samples, the guidelines of UNE-EN 13279–2:2014 standard [38] were followed, producing standardised RILEM samples measuring 40 × 40×160 mm^3, with a water/plaster weight ratio of 0.7. The water/plaster ratio was experimentally set according to the recommendations of the standard until a consistency of 165 ± 5 mm of the mixes was obtained by the vibrating table procedure.

Table 1
Main characteristics of the reinforced fibres used.

Type	Length (mm)	Bulk density (kg/m^3)	Modulus of elasticity (GPa)	Tensile strength (GPa)	Elongation to fracture (%)
Glass fibre	12	2680	72	1.70	4.30
Basalt fibre	12	2750	91	4	1.80

In this study, three groups of plaster composites have been considered.

In the first group, a series of plaster without additions was prepared, along with two series with partial substitution of the original raw material with 200 g and 400 g of dissolved EPS waste (DEW) respectively. The incorporation of DEW is carried out in the last stage of the mixing process, as shown in Fig. 1. This dissolution is obtained by the progressive incorporation of the solid EPS waste into the solvent with an EPS/solvent weight ratio of 1:2. The low polar chemical structure of the solvent gives it a high dissolving power over organic materials such as EPS [39], resulting in a homogeneous mixture with a density of 660 kg/m^3.

The second and third group of dosages have been carried out following the same process of partial replacement by weight of the original plaster material with DEW, adding glass fibre and basalt fibre as reinforcement, respectively. The amount of fibre used has been determined based on literature, where optimal results have been achieved with addition percentages around 1% of the total weight of the mixture [40], [22]. To ensure adequate distribution of the fibres in the composites, they were manually dispersed in the plaster powder prior to the mixing process [41]. Once hardened, all specimens were demoulded and cured in a laboratory environment for seven days at a temperature of 23 ± 2 °C and 50 ± 5% relative humidity.

In Table 2, the prepared composites have been named according to the following scheme: firstly, by referring to the base material (plaster) and the water/plaster ratio used (P0.7); then, the weight amount of original raw material replaced by DEW; and finally, the type of fibre incorporated, either basalt fibre (BF) or glass fibre (GF).

As can be seen in Table 2, the density of the composites significantly decreases as the proportion of DEW incorporated into the mixtures increases. Furthermore, the additions proposed in this research have led to a reduction in the amount of water and plaster that would have been necessary for the production of traditional plaster material, specifically, it has been possible to develop composites with a total saving of 24.5% in natural materials. In this way, it is possible to produce lightweight and more sustainable plaster composites, which can be used to manufacture prefabricated panels and plates. Therefore, this work aligns with the objectives outlined in the European Green Deal [42], to steer the construction sector towards a circular economy model that is committed to the recovery and revaluation of construction and demolition waste.

2.3. Tests procedures

The effects of fire in buildings vary greatly depending on the characteristics of the existing fire load (type and quantity of fuel, configuration and distribution of the fire), as well as the ventilation conditions of the space where it occurs [43]. Considering this, a non-standardised direct real-fire test has been conducted at Collado Villalba Fire Station (Madrid, Spain), developed by Serrano Somolinos in his doctoral thesis [23]. This test aims to reproduce the effects that the development of a real fire would have on a material, adapting the ISO 834–1:1999, UNE-EN 1363–1 and UNE-EN 1363–2 standards [44],[45],[46].

Prior to the test, the samples were dried in an oven for 24 h at a temperature of 40 ± 2 °C and 50 ± 5% relative humidity, in order to stabilise the mass of all samples and to remove any free kneading water that may have remained inside the composites. Then, the samples were horizontally distributed on a 1 m^2 steel grid, so that the different elaborated composites were homogeneously distributed on the surface, as shown in Fig. 2. At all times, a free space of 4 cm was ensured between the samples, thus guaranteeing the maximum contact between the samples and the fire.

The test was conducted for 30 min with a calorific potential of 20 kg of pine wood [47]. To initiate ignition, the wood was evenly sprayed with gasoline, and once the wood combustion was complete, the samples were allowed to cool to ambient temperature. During the test, the surface temperature of the samples was recorded with a Testo 845 infrared thermometer and infrared images were taken with a FLIR E40bx

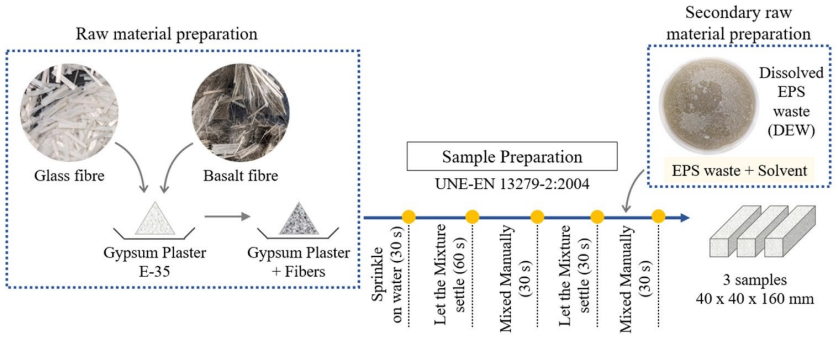

Fig. 1. Schematic diagram of the specimen production process.

Table 2
Dosages, bulk density and original raw materials savings of the produced composites.

Type	Plaster (g)	Water (g)	DEW (g)	GF (g)	BF (g)	Bulk density (kg/m^3)	Raw material sustitution (%)
P0.7	1000	700	_	_	_	1104.6	0.0
P0.7-200	883	617	200	_	_	935.3	11.8
P0.7-400	765	535	400	_	_	850.2	23.5
P0.7-BF	990	693	_	_	17	1075.8	1.0
P0.7-200-BF	872	611	200	_	17	893.2	12.8
P0.7-400-BF	755	528	400	_	17	825.6	24.5
P0.7-GF	990	693	_	17	_	1091.3	1.0
P0.7-200-GF	872	611	200	17	_	861.1	12.8
P0.7-400-GF	755	528	400	17	_	837.6	24.5

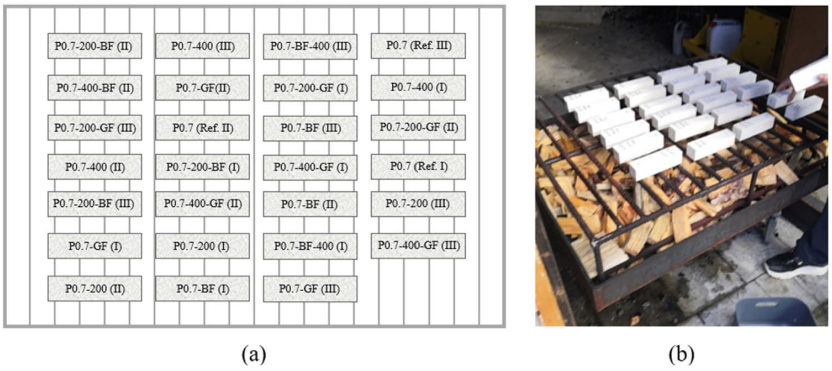

Fig. 2. (a) Diagram of the distribution of the samples on the grid, (b) Placement of the samples for the test.

Fig. 3. Images of the direct fire test: (a) Start of test, (b) Test development, (c) Cooldown.

camera. It should be noted that, in this test where the aim was to replicate a real fire situation, wood combustion can occur unevenly across the grid surface (Fig. 3). Therefore, three temperature measurements were taken on each sample every five minutes, in order to determine the fire behaviour curves of each produced composite.

After the real direct fire test, the mechanical characterisation of the new plaster composites was carried out by means of surface hardness, flexural strength and compressive strength tests, following the specifications of the UNE-EN 13279–2:2014 standard [38]. Surface hardness was obtained using a Shore C hardness tester, taking five measurements on two opposite longitudinal faces of the samples. Flexural and compressive strength tests were performed using an IBERTEST AUTOTEST 200–10SW press until the samples broke. Both the series of composites subjected to the real direct fire test and another series of three reference specimens for each proposed dosage were tested to compare the obtained results. Additionally, to enrich the discussion of the results, images were obtained using scanning electron microscopy (SEM) for both the reference composites and the composites subjected to the fire test. A Jeol JSM-820 microscope operating at 20 kV, equipped with Oxford EDX analysis, and a Cressington 108 metalliser for sample preparation were used to obtain these SEM images.

Furthermore, the physicochemical characterisation of the new plaster composites developed was carried out by performing X-ray diffractogram (XRD) and thermogravimetric analysis (TGA) tests. Since the preparation of the samples for these tests requires a specific grinding and sieving process, it is not possible to preserve the fibres in the samples, so only the composites that did not contain fibres were analysed. XRD was conducted using a Siemens Krystalloflex D5000 with a Cu-Kα graphite monochromator. The range used was between $5° \leq 2\theta \leq 60°$ every 0.04° and 4 s per step. The International Centre for Diffraction Data Powder Diffraction Files (ICDD PDF) database was employed to identify the composition of the samples. Once the diffractograms were obtained, the mean size (D) of the ordered crystalline domains in the samples was calculated, using the Debye-Scherrer Eq. (1):

$$D = \frac{k\lambda}{\beta \cos\theta} \quad (1)$$

where D is the mean size of the crystallite (nm), k is the Scherrer constant taken as 0.94, λ is the wavelength of the Cu-Kα radiation (0.154056 nm), β is the Full Width at Half Maximum (FWHM) of the X-ray peak in radians and θ is the Bragg angle also in radians [48]. The FWHM has been calculated using the most intense peak of calcium sulfate dihydrate at $2\theta = 20.742°$. On the other hand, for the TGA analysis, a TA Instruments SDT Q600 was used, with a heating rate of 10 °C/min. The test started at room temperature until a temperature of 1000 °C was reached in a pre-filtered air atmosphere with a flow rate of 100 ml/min.

Finally, the total organic carbon (TOC) content of the composites was determined using the total combustion method [49]. For this purpose, an elemental analysis was carried out by combustion of each composite sample at 950 °C in a controlled O_2 atmosphere using a LECO TruSpec Macro CHN elemental analyser. All carbon forms CO_2, which is measured by a non-dispersive infrared (NDIR) detector, with the amount of CO_2 in the sample being directly proportional to the amount of carbon present. The TOC concentration was obtained by the differential method, which consists of determining the total carbon (TC) and the inorganic carbon (IC) and then calculating the total organic carbon content by difference, according to Eq. (2):

$$TOC = TC - IC \quad (2)$$

For the calculation of CI, part of the sample is first calcined at 550 °C for 6 h, removing organic matter and then subjected to combustion. Once the TOC of the composites was obtained, it was possible to calculate the theoretical emissions of carbon monoxide and carbon dioxide associated with the combustion of the new plaster composites developed under conditions of a potential fire. To calculate the gas emissions, a standard room of $3 \times 4 \times 2.6$ m^3 was considered in which false ceiling panels measuring $600 \times 600 \times 12.5$ mm^3 made with the plaster composites developed in this research were installed.

3. Results and discussion

This section presents the results derived from the experimental campaign proposed, which includes both the direct real-fire tests of the different plaster composites produced, as well as their subsequent mechanical and physicochemical characterisation.

3.1. Direct real-fire test

The results of this test have been represented as time-temperature curves for each type of plaster composite. To facilitate the analysis and discussion of this test, these curves have been grouped according to two criteria: (1) based on the type of the added reinforcement fibre (Fig. 4(a), (b) and (c)) and, (2) depending on the amount of original raw material replaced by DEW (Fig. 4(c), (d) and (e)). It should be noted that at the start of the test, the average surface temperature of all the specimens was 13.5 °C.

In Fig. 4(a), it can be observed that in all samples, the temperature increases rapidly during the first five minutes of the test, reaching the maximum temperature peak at around ten minutes, as in other similar studies [17,47]. The plaster without additions (P0.7), reached the highest temperature (472 °C), while the composites with DEW addition recorded a slightly lower temperature. Specifically, the P0.7–400 composite reached the lowest maximum temperature during the test (431 °C). After ten minutes, the samples started to cool down gradually, reaching a temperature of around 300 °C after 20 min of exposure. At the end of the test, the P0.7 plaster retained the most heat (279 °C), while the P0.7–400 composite, with the highest amount of DEW in its composition, had the lowest temperature (239 °C).

As shown in Fig. 4(b), the composites with basalt fibre addition also reached the maximum temperature peak at ten minutes, with P0.7-BF composite recording the highest temperature (502 °C). The P0.7–400-BF plaster experienced the lowest temperature rise, reaching a maximum temperature of 453 °C. Unlike the previous case, the basalt fibre composites experienced a slower cooling, not reaching 300 °C until after 25 min. At the end of the test, the P0.7–200-BF composite experienced a more gradual cooling, retaining the highest temperature at the end of the test (302 °C). The P0.7-BF plaster experienced the most abrupt cooling after the flame was extinguished, at 15 min.

Fig. 4(c) shows how the plaster with glass fibre (P0.7-GF) reached the highest temperature, 458 °C, however, the P0.7–400-GF composite obtained a similar peak temperature (455 °C). Likewise, the P0.7-GF plaster was the composite that cooled the slowest, recording 291 °C at the end of the test. Both DEW composites behaved similarly during cooling, reaching temperatures around 235 °C after 30 min.

As shown in Fig. 4(d), in the composites without DEW addition, the highest temperature was reached in the composite with basalt fibre P0.7-BF, followed by the plaster without additions (P0.7) and the composite with glass fibre P0.7-GF, with temperatures of 502 °C, 472 °C and 458 °C respectively. After reaching the temperature peak at ten minutes, the samples with basalt fibre experienced the slowest cooling, although at the end of the test all the samples recorded similar temperatures, around 290 °C.

The behaviour of the composites incorporating 200 g of DEW is presented in Fig. 4(e). Again, the composite with basalt fibres (P0.7–200-BF) exhibited the most rapid temperature increase during the initial five minutes, reaching the highest temperature (493 °C) at ten minutes of fire exposure. Plasters P0.7–200 and P0.7–200-GF reached a similar maximum temperature, around 441 °C. Composite P0.7–200 began cooling down more quickly, although, after 20 min of testing, composite P0.7–200-GF experienced an abrupt cooling, reaching a final

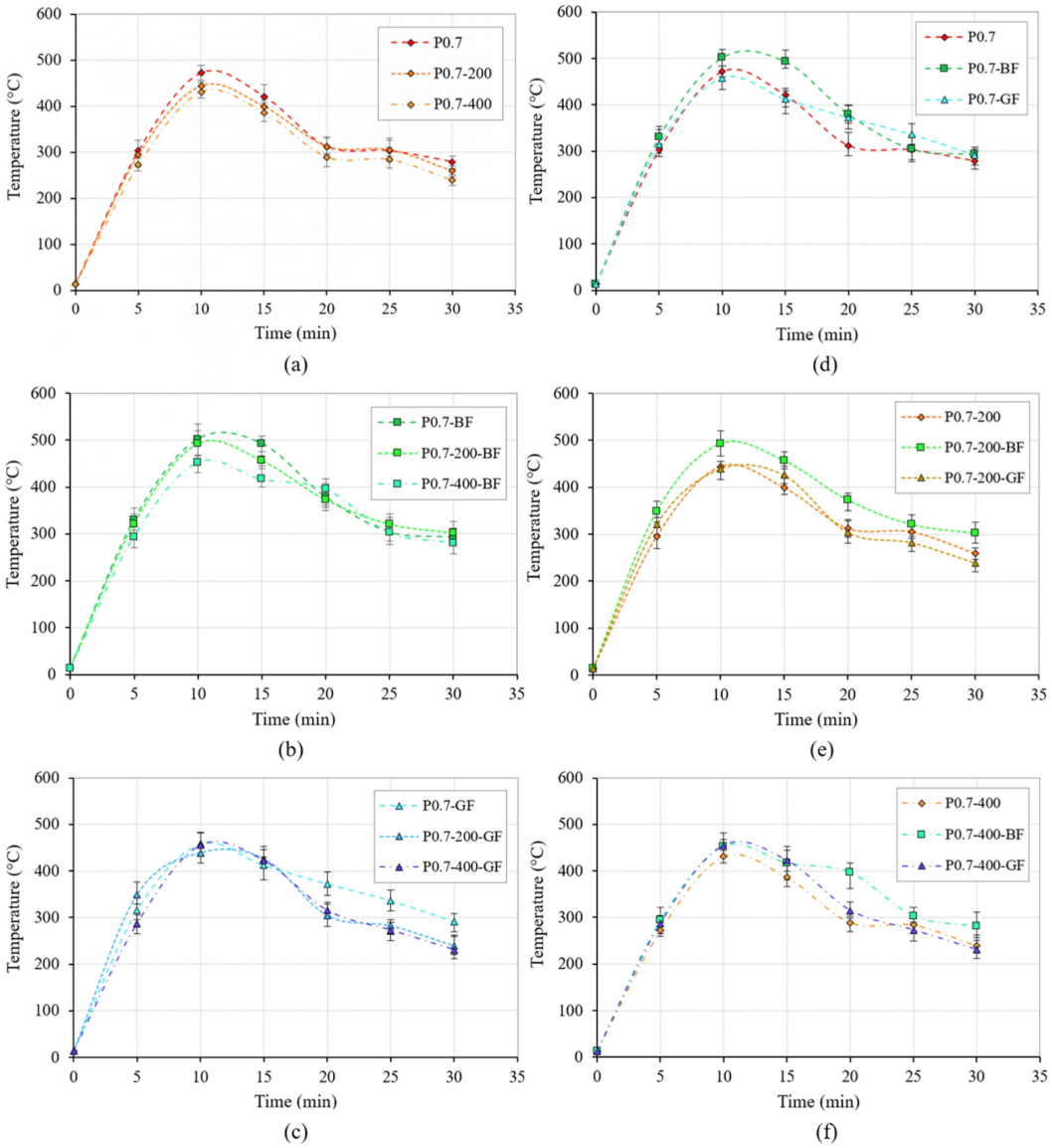

Fig. 4. Mean time-temperature curves achieved by samples during the direct real-fire test: (a) Composites without fibres; (b) composites with basalt fibre; (c) composites with glass fibre; (d) composites without addition of DEW; (e) composites with 200 g of DEW; (f) composites with 400 g of DEW.

temperature of 239 °C. Composite P0.7–200-BF underwent a gradual cooling, retaining the highest temperature at the end of the test.

Finally, Fig. 4(f) presents the temperature curves of the composites incorporating 400 g of DEW. It can be observed that, at the beginning of the test, all the compounds show similar laws of development, reaching around 385 °C in the first five minutes. The highest temperature was recorded for the plaster P0.7–400-GF, with 455 °C. After 15 min, the cooling phase started for all samples, however, the dosage with the addition of basalt fibres (P0.7–400-BF) maintained a higher temperature after 20 min, while the composite without fibres, P0.7–400, experienced the fastest cooling.

Ultimately, the composites with the addition of basalt fibres experienced a faster rate of temperature rise, as well as a higher peak temperature after ten minutes of testing. These results agree with other studies where it was observed that basalt fibres heated up more rapidly, reaching higher temperatures compared to glass fibres due to their higher thermal emissivity [50]. In general terms, composites with glass fibre incorporation experienced faster cooling than the rest of the composites, resulting in lower temperatures at the end of the test [51]. In all cases, it can be observed that the heating process of the samples is noticeably slower the higher the proportion of DEW in the mixtures, leading to lower peak and final cooling temperatures compared to the composites without DEW. As indicated in Table 2, the increase in porosity as a consequence of the decrease in density of the plaster composites incorporating DEW [52], as well as the voids left by the residue in the matrix after reaching its decomposition temperature [53], leads to lower temperatures as the pore network favours the transmission and release of the water vapour produced inside the composites,

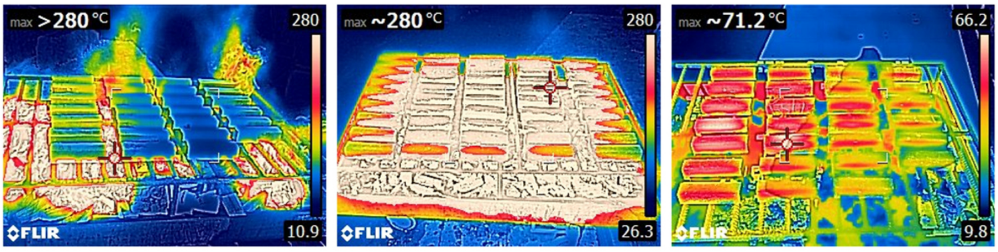

Fig. 5. Thermographic images of the direct live fire test: (a) Start of combustion, (b) End of combustion, (c) Cool down.

thus reducing the pressure inside the matrix and preventing the cracking of the material [54].

In Fig. 5, some thermographic images captured during the test are displayed. These images show the temperature and initial arrangement of the composites on the test grid (Fig. 5(a)), an image captured after the end of the test that replicates the conditions of a direct real-fire (Fig. 5 (b)), and, finally, an image of the cooling process after the flame has been extinguished after 30 min of the test (Fig. 5(c)).

Finally, to complete the discussion of the results obtained in this test, Table 3 shows the fire severity obtained from the area under the time-temperature curve of each of the prepared composites. In addition, Table 3 also includes the variation in the mass of the samples tested before and after exposure to direct real-fire.

As can be seen in Table 3, the introduction of fibres increased the fire severity by 10.42% in the case of basalt fibres and by 4.5% with glass fibres compared to the reference plaster (P0.7). In all cases, increasing the amount of DEW added proportionally reduced the intensity of the fire action, with the P0.7–400 composite experiencing the lowest fire severity. Furthermore, Table 3 shows that the introduction of fibres in the traditional plaster leads to a reduction in mass loss after the fire test, being more significant with glass fibres. However, the greatest mass loss is observed in the cases where partial replacement of the original plaster material with DEW was carried out, becoming more relevant as the amount of recycled material in the mixtures increases.

3.2. Mechanical characterisation

In this section, the results of the mechanical characterisation of the different plaster composites developed in this research are presented. Thus, the residual mechanical capacity of the samples exposed to direct real fire test has been determined and compared with the values obtained for the reference series of each composite designed without exposure to the severity of this external agent. Fig. 6 shows the results obtained after the flexural strength test.

In Fig. 6, it can be seen that all the reference composites exceeded the minimum value of 1 MPa for the flexural strength set by the current standard. In the specific case of the plaster composites without fibres, the P0.7–200 sample showed an increase in strength of 10.47% with respect to the P0.7 composite. However, in line with previous studies [12], it is observed that increasing the amount of recycled material added to the plaster composites leads to a decrease in mechanical strength. Additionally, it is noted that the incorporation of reinforcement fibres in the matrix of the composites improves the flexural strength, with this increase being more significant in the case of the samples with glass fibre [20].

On the other hand, all the series of composites exposed to the action of fire experienced a reduction in strength, with a marked decrease in the mechanical capacity of the composites without fibres. The plaster without additions (P0.7) could not be tested after being subjected to the action of direct real fire as a consequence of shrink and crack due to the dehydration process that this type of construction material undergoes when subjected to high temperatures [55]. This dehydration breaks down the plaster crystals in the matrix of the composite, weakening the material [56]. Otherwise, all the composites reinforced with glass or basalt fibres reached values above the minimum indicated by the current standard UNE-EN 13279–2:2014 [38]. Nevertheless, as demonstrated by Li *et al.* in their study [21], basalt fibres experience a reduction in their mechanical strength at temperatures above 300 °C, therefore, after the fire test conducted, where temperatures above 400 °C were reached, glass fibres proved to be more efficient in preserving the flexural strength [20].

The new lightened plaster composites with the addition of DEW showed in all cases higher flexural strength values than the plaster P0.7 after being subjected to the action of fire. In the case of the composites with the incorporation of basalt fibres, the flexural strength after the fire test was 57.52% and 15.69% higher in the P0.7–200-BF and P0.7–400-BF composites, respectively, compared to the plaster material without the incorporation of DEW. On the other hand, samples with glass fibre incorporation reported the highest strengths after fire exposure, although there is a proportional decrease in flexural strength as the amount of DEW added as a partial replacement of the original plaster material increases. Thus, contrary to what has been observed in other investigations, where the addition of granulated plastic waste results in the disintegration of the plaster samples [17], the new composites developed showed on average good dimensional stability and acceptable mechanical flexural strengths after exposure to real fire conditions.

Next, Fig. 7 presents the results obtained in the compressive strength test and Shore C surface hardness of the composites subjected to the fire test and the reference composites.

After analysing Fig. 7, it can be seen that in the series not subjected to

Table 3
Fire severity during direct real-fire test and mass loss of composites.

Type	Fire severity (°C min)	∇mass after fire (%)	Type	Fire severity (°C min)	∇mass after fire (%)	Type	Fire severity (°C min)	∇mass after fire (%)
P0.7 (Ref.)	9786.25	16.18	**P0.7-BF**	10806.25	14.84	**P0.7-GF**	10226.25	14.57
P0.7-200	9456.25	20.47	**P0.7-200-BF**	10613.75	18.71	**P0.7-200-GF**	9631.25	17.95
P0.7-400	8941.25	25.93	**P0.7-400-BF**	10051.25	25.74	**P0.7-400-GF**	9371.25	24.45

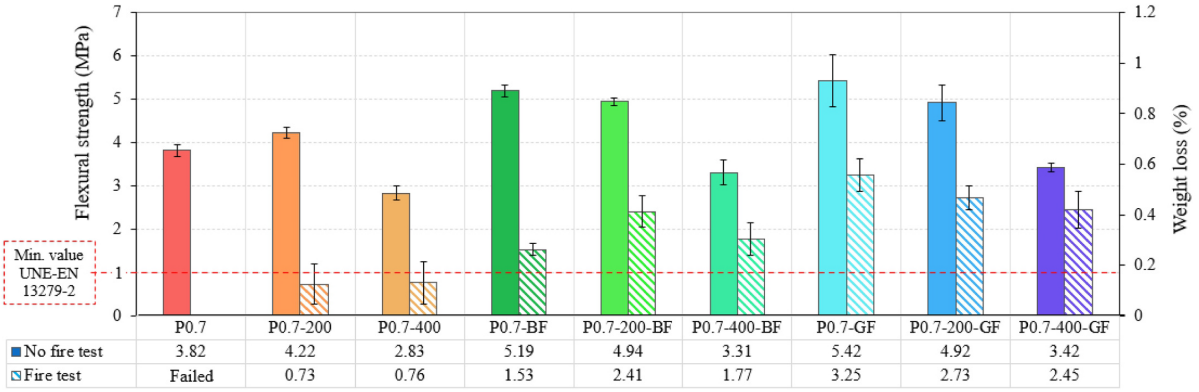

Fig. 6. Flexural strength of the different plaster composites produced. The solid and grated bars correspond to the reference and those subjected to fire, respectively.

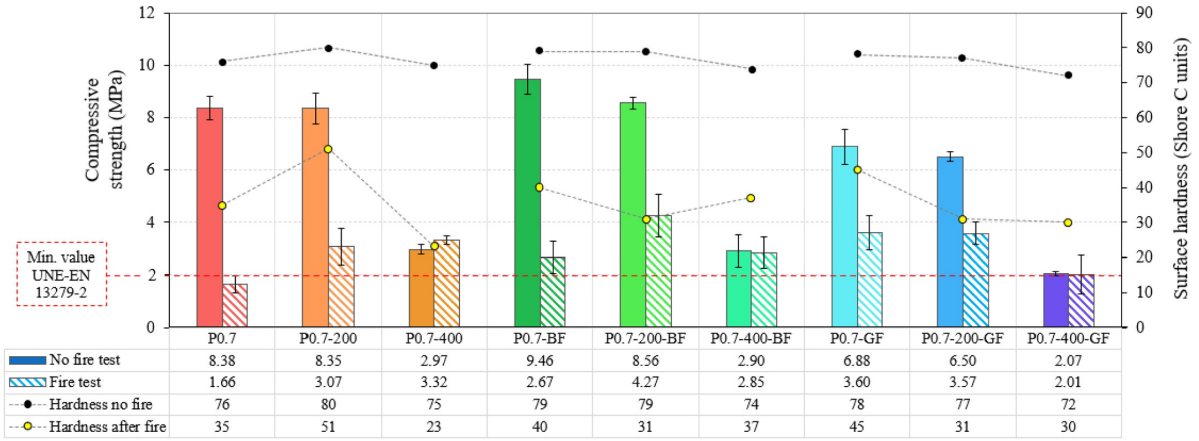

Fig. 7. Results of the compressive strength and Shore C surface hardness test of the reference composites (solid patterned bars) and those subjected to direct real fire test (grated patterned bars).

fire, the incorporation of DEW in the composites slightly reduced the compressive strength, with a more significant decrease in the series with a greater incorporation of recycled material. However, all the composites included in this study met the minimum 2 MPa required by current standards [38]. While it is true that the incorporation of fibres in the matrix does not necessarily have a significant impact on the compressive strength of plaster composites [57], an increase in strength of 12.89% was observed in this study with the addition of basalt fibres. However, in composites with glass fibre, there was a slight decrease in compressive strength of 17.80% compared to plaster without additions.

Once subjected to the effect of high temperatures, the composites with the addition of DEW without reinforcement fibres recorded higher compressive strengths than those obtained with traditional plaster (P0.7), reaching an average of up to 1.66 MPa more in the case of the P0.7–400 composite. It should be noted that the plaster without additions was the only one that did not reach the minimum strength of 2 MPa after the fire test. Some authors have already pointed out how density reduction in lightweight plasters can benefit the compressive strength after reaching temperatures around 600 °C [20]. On the other hand, in samples reinforced with basalt fibre, the addition of DEW increased the post-fire strength, being more relevant in the P0.7–200-FB composite with a 59.93% increase compared to the P0.7-BF composite. In composites reinforced with glass fibre, the opposite behaviour was observed, with compressive strength worsening as the amount of DEW in the mixtures increased. Nevertheless, in the samples without incorporation of recycled material, it can be observed how the addition of glass fibre reinforcement experiences a lower initial strength loss after exposure to fire, due to the higher absorptivity of the basalt fibres [51].

Regarding surface hardness, Fig. 7 shows that the incorporation of DEW in the matrix of the plaster composites resulted in a slight decrease in the Shore C hardness values. On the other hand, the incorporation of reinforcing fibres in the plaster materials did not lead to any significant improvement in surface hardness values, as had been observed in other studies [58]. Furthermore, after being subjected to the action of fire, all the composites produced experienced a decrease in their surface hardness, with the samples with higher DEW incorporation in their composition being more affected.

Finally, in order to further study the behaviour of the new composites produced after being subjected to the direct real fire test, Fig. 8 shows images obtained by scanning electron microscopy (SEM) of samples P0.7, P0.7-GF and P0.7–400-GF. These composites were selected as representative samples due to the significant differences between them among all the mixtures elaborated. In addition, as the samples with glass fibre showed the highest flexural strength after the fire effect, it is considered that these composites would be more viable for use in the production of new sustainable lightweight prefabricated construction products.

Fig. 8(a) and (c) (P0.7 and P0.7-GF composites, respectively) show

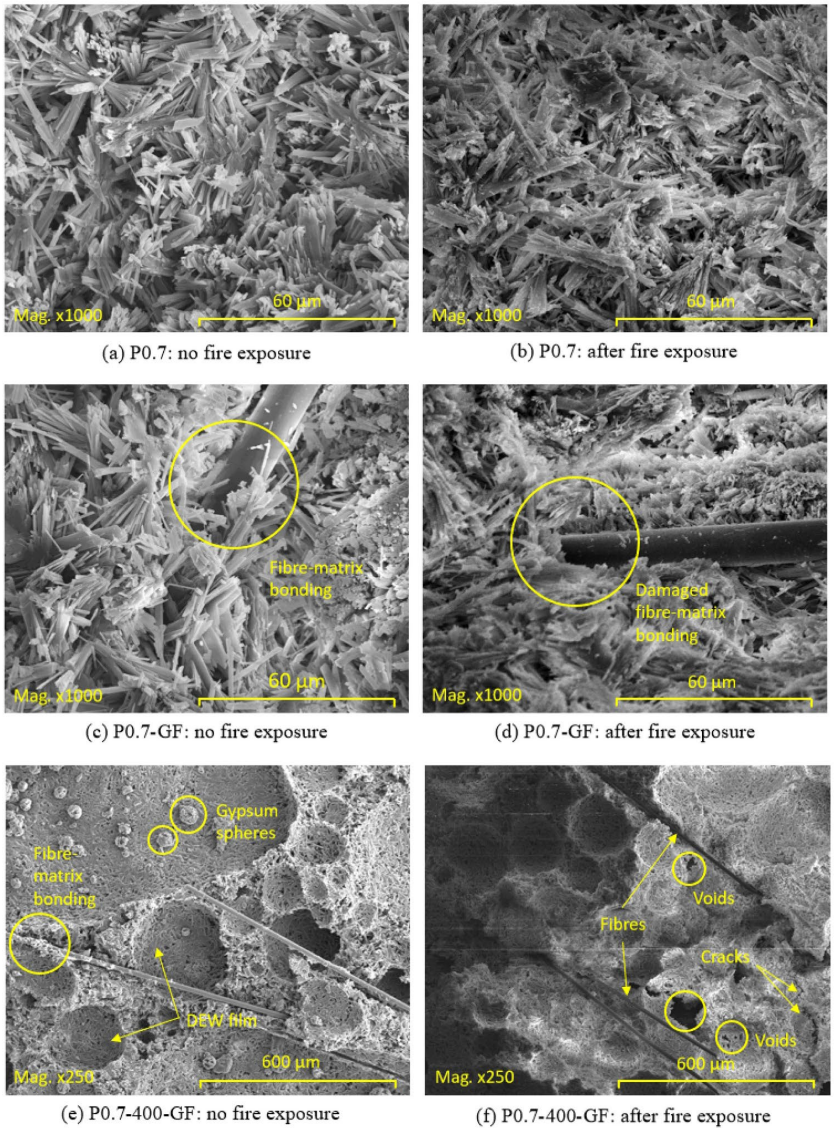

Fig. 8. SEM images of the composites P0.7, P0.7-GF and P0.7–400-GF.

the characteristic granular texture based on acicular crystals composed of calcium sulphate dihydrate, which are common in plaster [59]. This indicates that the addition of the fibres did not lead to substantial alterations in the formation of the internal structure of the composites. Moreover, the plaster crystals surrounding the fibres at the matrix-fibre interface in Fig. 8(c) suggest a good connection between both materials.

Fig. 8(e) shows how the incorporation of DEW produced high porosity in the composites, with the solidified EPS adhering to the walls of the pores and covering the gypsum crystals, which would limit their growth [60]. The spherical structures present on the matrix indicated in Fig. 8(e) would promote a decrease in interlocks between crystals, and, therefore, a reduction in the mechanical strength of these composites.

In Fig. 8(b), (d) and (f) the destructive action of fire on the plaster matrix is clearly visible. The crystals show significant deterioration due to the degradation suffered after exposure to temperatures above 400 °C [16]. Additionally, the loss of cross-section and shortening of the crystals after exposure to fire reduced the contact surface area between fibres and matrix, as shown in Fig. 8(d), leading to a substantial strength loss observed in the mechanical tests. However, the fibres still retained their integrity, showing high stability after being subjected to high temperatures.

Lastly, Fig. 8(f) shows that the DEW present in the P0.7–400-GF plaster has completely decomposed, since the degradation temperature of the EPS begins around 300 °C [61]. The spheres composed of gypsum crystals that were observed in the reference composite (Fig. 8(e)) also disappear after the fire, which suggests that these structures were formed by the effect of DEW in contact with the crystals. In general, a rather degraded matrix appears, with several voids and microcracks that reduce the interlocking microstructure of the composite. However, the ability of DEW to create of pathways after its degradation, through which high pressure vapour can be released, favours the preservation of the mechanical strength of the composites after the action of fire [20,